rotec GmbH

Prüfsysteme für den Maschinenbau

Applications and Publications

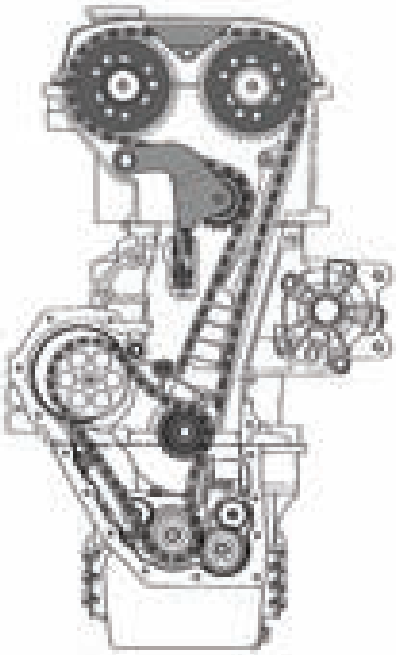

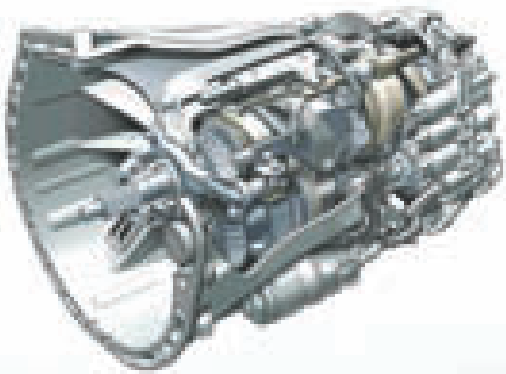

www.rotecmunich.de

Contents

Experimental Valvetrain Analysis

Porsche Engineering Services, Bietigheim-Bissingen

Development engineers are increasingly focusing on control of the gas exchange cycle because of its influence on the mixture formation and combustion processes.

Besides direct injection, the valvetrain still offers much potential for optimising modern petrol engine combustion characteristics.

Development aims are geared towards improving control of variable valve timing on the one hand and improving the dynamic characteristics of both the valvetrain and cam drive on the other. The latter is of particular interest to manufacturers of high-performance engines. In valvetrain engineering, optimum gas dynamics would be achieved with instantaneous opening to maximum lift followed by instantaneous closure at all engine speeds. In this way maximal integral areas under the valve lift curves are provided by the shortest possible opening durations.

This results in high levels of structural excitation with components being subject to significant stresses which increase as a function of the square of the speed. The development tasks are to design lifetime-long, maintenance-free valvetrains which satisfy all acoustic, cost and manufacturing requirements.

Porsche Engineering investigates the basic design and functionality of the valvetrain on motored test rigs. The use of expensive, fired engine tests is avoided in the early stages of the development process in order to shorten development time and reduce costs. Measurements on fired engines are only performed when satisfactory results for valvetrain kinematics and stresses over the complete speed range have been achieved in the rig tests.

The entire valvetrain system can be reproduced on the test rig. Oil pressure, temperature and aeration levels approaching those expected on the fired engine may be obtained. A high-performance asynchronous drive allows comprehensive investigation of effects such as tooth backlash, tooth pitch error, chain drive polygon effect, damping influence of hydraulic chain tensioners and variable camshaft torques. Fired-engine operating conditions are approached including expected rotational speed fluctuations of the crankshaft.

These circumstances require dynamic, non-intrusive measurement with high resolution for which a non-

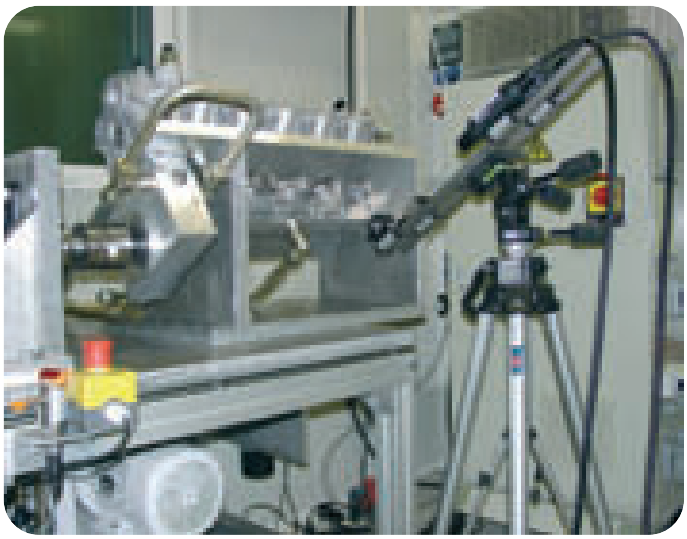

Figure 1 *Test bench with Porsche Carrera GT cylinder head and non-contact laser measuring system*

contact, optical measuring system is most appropriate. The laser system used by Porsche Engineering allows for independent measurement of both valve lift and velocity. Displacements and velocities of up to 160mm and 30m/s respectively may be measured. A differential measurement principle ensures that any vibration of the test setup is detected and compensated. In addition, incremental rotary encoders are used for determining rotational speeds and angular positions of shafts.

Dynamic signals require an extremely fast dynamic data acquisition and analysis system for synchronous acquisition of all signals. The hardware and software architecture of the Rotation Analysis System (RAS) from Rotec GmbH is most suitable for the tasks at hand. The RAS hardware samples the analogue laser signals at 400kHz per channel and can acquire rotary encoder signals up to 1MHz pulse frequency. The RAS software allows for quick, user-friendly analysis with a customised valvetrain program including temperature compensation, non-linear response and offset correction for valvelift sensors.

Typical analyses include:

- Measured valve lift and velocity versus camshaft speed and angle
- Valve acceleration, deceleration and bounce
- Valve timing (open, close and duration)
- Comparison of measured data with theoretical curves

Thanks to this measuring technology the effects of different valvetrain parameters e.g.: cam profiles, spring stiffnesses, valvetrain masses etc. can be easily determined at an early stage in the development cycle on the test rig without the test engineer having to make cumbersome adjustments to the engine itself. The influence of any modifications made can be seen in the measured valve closing velocities and valve accelerations and by referring to the calculated contact forces and hertzian stresses. Torsional vibration analysis also provides useful information on valvetrain operational behaviour.

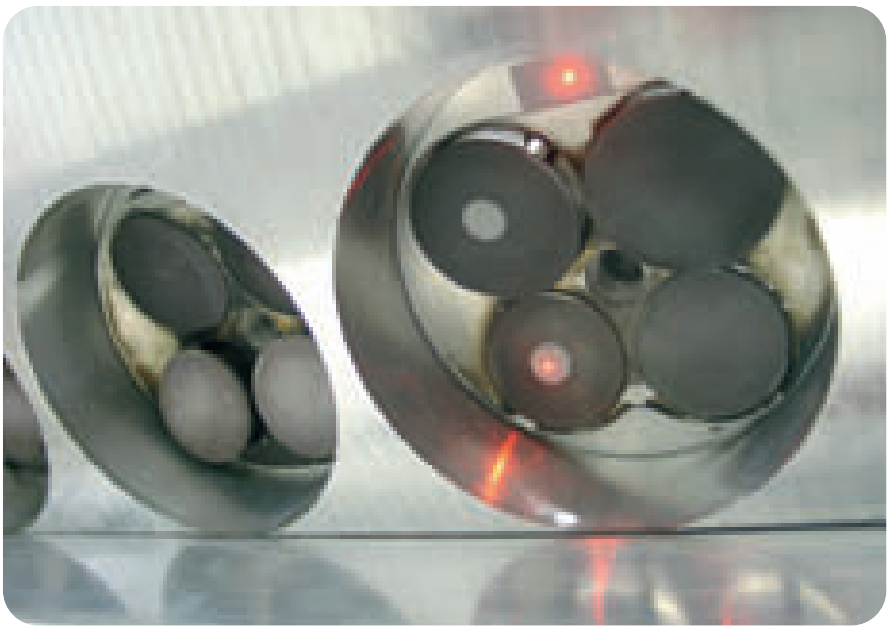

Figure 2 *Valve head and reference point with laser beam for differential measurement*

As a leading provider of engineering services, Porsche Engineering undertakes development work for other automotive companies. The trend towards shorter development cycles combined with the increasing complexity of val-

vetrain systems should make the valvetrain testing expertise described here of particular relevance to engineers involved in engine development.

The development of the Porsche Carrera GT V-10 Engine is a recent example of a successful application of the valvetrain testing technology described here. The aim was to understand the valvetrain system and implement improvements at an early stage thus avoiding expensive, time-consuming development loops.

Performing effective experimental valvetrain analysis in engine development reduces costs, saves time and minimises risk for the customer.

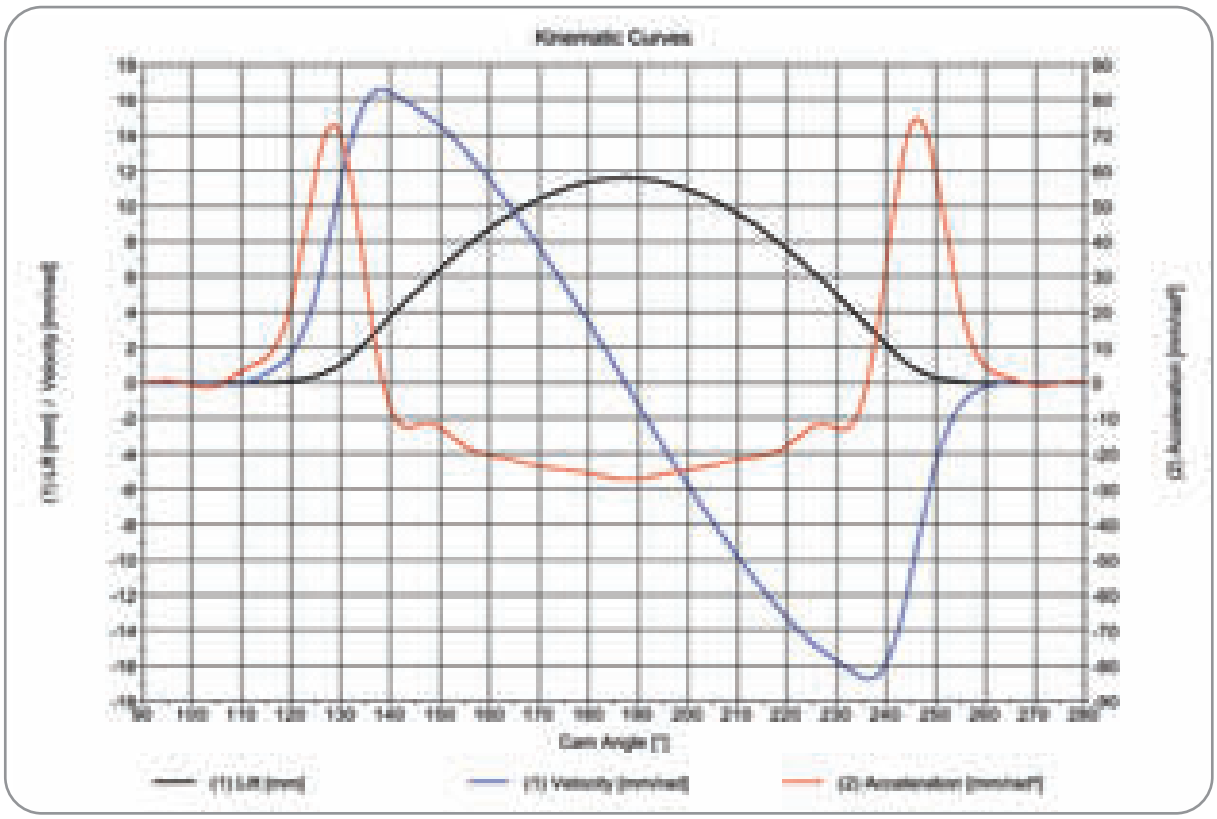

Figure 3 *Kinematic analysis of valve lift, velocity and acceleration. The kinematic, kinetic and dynamic behaviour of the valvetrain is determined from both these curves and from further measurements and calculations.*

Experimental Valvetrain Analysis
Porsche Engineering Services, D-Bietigheim-Bissingen. From »Testing Technology International, September 2004.«

New Equipment and Methodology to Perform High Speed ValveTrain Dynamics Testing and Analysis

Jeff G. Sczepanski, Ford Motor Company, Detroit

Abstract

With the increased need for variable and high-speed valvetrains for improved performance and economy, greater importance must be placed on valvetrain testing and prove-out. To make an accurate assessment of valvetrain capability and high-speed dynamics, improved test and analysis capability is needed.

The objective of this paper is to provide the necessary information for others to understand and perform high-speed valve train dynamics testing using current state-of-the-art equipment. It includes the use of a differential laser vibrometer to measure complete valve lift and velocity and a Rotational Analysis System (RAS) that easily and quickly reduces the data to plots and compares measured valvetrain dynamics to theoretical models. Also covered are valve closing velocity measurements, calculated valve accelerations, torque, torsional vibration, sample rate and filtering. Effects of torsional vibration, sample rate and filtering on measurements are also demonstrated.

Introduction

Until recently, valvetrain dynamics testing was restricted to the use of proximity probes, strain gauges and other instrumentation that are difficult to install, have limited frequency range for to obtain complete valve dynamics information [1-4]. Often, time based measurement systems are used that infer shaft position (ignoring shaft dynamics) by interpolating shaft angle over time for one revolution, or use angular sampling while ignoring angular position over time. Some of these data acquisition instruments multiplex measurements, rather than collecting data synchronously. These methods can miss the driveline dynamics that affect valvetrain performance or add additional time errors when relating data between channels. Most testing and analysis is being done with unrelated equipment, with each portion of the system having its own limitations, resulting in filtered data that represents snap-shots in time, making it difficult to understand complete valvetrain dynamics.

Modern state-of-the-art equipment is a requirement to support on going programs including increasingly complex mechanical variable valve lift and valve deactivation systems. Two key pieces of equipment and software are needed to do this. The first piece of equipment was used to measure full valve motion and the second to measure data with respect to shaft position and time. Software was also needed to process and analyze the dynamics. The goal was achieve significantly higher throughput with real time analysis capabilities.

New Equipment And Methods For Walvetrain Testing And Analysis

The writer believes this to be the first application of two unique pieces of state-of-the-art equipment that provide dramatic insight into valvetrain dynamics. The first is Polytec PI's High Speed Laser Vibrometer (HSV). This instrument is capable of measuring differential valve lift and velocity (up to 30m/s) and can measure speeds in excess of most, if not all, types of motor-sports applications. Its high bandwidths (250kHz for lift and 50kHz for velocity) greatly improve the information gained from valve acceleration calculations. The second is a Rotec GmbH Rotational Analysis System (RAS). It is capable of measuring 40-bit time-based angular camshaft position and relating this to its analog measurements on a time, angle or speed axis. It has 400kHz data acquisition cards for high-speed dynamics measurements. It includes near real-time software, which provides extensive analysis capabilities including newly developed tools for valvetrain analysis (valve timing and closing velocity). The RAS can automatically interpolate between data points and has many other features, including torsional vibration modeling capabilities.

This paper covers test configuration, instrumentation and data acquisition, test parameters, measurements, analysis, and conclusions. Greatest emphasis is placed on the analysis section that includes speed control, valve lift and timing, valve velocity, valve acceleration, cam torque and power, torsional vibration, rocker strain, filtering and sample rate.

The test data in this paper is from either a production I4 Variable Valve Lift (VVL) RFF cylinder head or a Ford V6 RFF cylinder head. These cylinder head bench tests were performed at different locations with different drive system configurations and dynamic characteristics. The VVL head was thoroughly tested at each of six different valve lifts and with manually controlled valve lift sweeps.

Test Configurations

Figure 1 is the VVL cylinder head bench test block diagram. It has a 1-1/2 inch long, _ inch diameter shaft off the flywheel and a 6-inch long, _ inch diameter shaft to the camshaft and a 15 HP motor. Figure 2 is a picture of the VVL cylinder head with the cam encoder, control shaft potentiometer, manual control shaft lever and control shaft motor location from left to right. The V6 cylinder head test configuration is similar in appearance to Figure 1 except that it has an additional coupling between the motor and flywheel, the flywheel is half the thickness, it's driven by a high inertia 190hp motor, the encoder is mounted to the back end of the motor shaft and it uses one inch

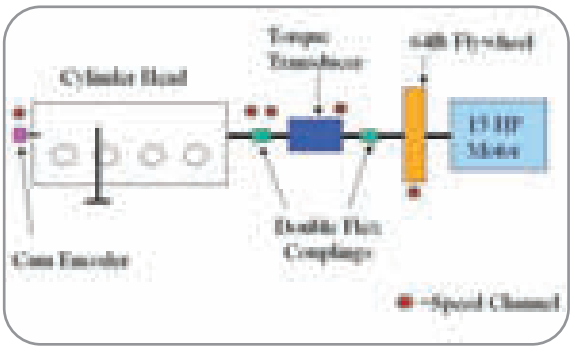

Figure 1 *VVL Bench Test Configuration*

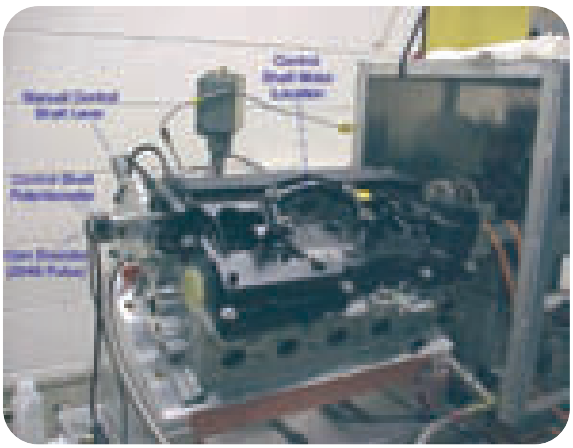

Figure 2 *VVL cylinder head on test bench*

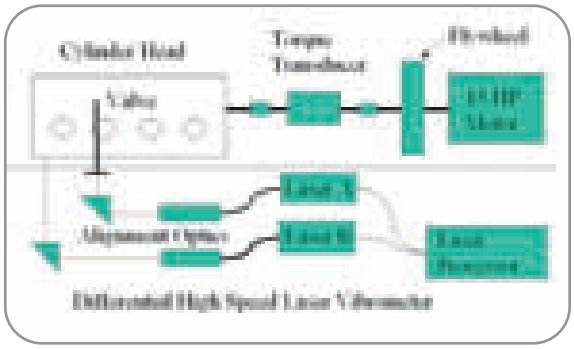

Figure 3 *Differential Laser Vibrometer layout*

shafts, with three double flex couplings and has a total length of approximately 36 inches.

Figure 3 is a block diagram showing the differential capabilities of the HSV. Laser A measures the valve motion and laser B the head motion. It has outputs for A or A-B displacement and A, B and A-B velocity. B displacement was measured with an optional external displacement decoder.

Instrumentation and Data Acquisition

VVL I4 Cylinder Head Instrumentation

The VVL test cell used the following instrumentation:

- Polytec PI HSV 2002A, HSV-AK 800, VEX 030 (Differential Valve Lift & Velocity)
- Heidenhain ERN1020 2048 Pulse optical encoder (camshaft position)
- Potentiometer: Novotechnik SP2831 A582 (Variable valve lift control shaft position)
- Torque Sensor: Lebow, 1604-500inlb (also 1104-200, 1104-500 and 1604-1000inlb)
- RAS laser speed sensors

Ford V6 Cylinder Head Instrumentation

The V6 cylinder head test cell included the following instrumentation:

- Polytec PI HSV 2002A (Valve Lift & Velocity)
- Kistler 360 pulse Optical Encoder (motor position)
- Torque Sensor: Lebow, 1104-500inlb
- RAS laser speed sensors (cam coupling position)

Data Acquisition and Post Processing

Measurements were taken on both cylinder heads using the RAS. This system has many hardware and software features to simplify the test cell setup and provide quick analysis. Some of the hardware features used were:

- 10GHz 40-bit speed channels that time stamp the leading edge of the encoder pulses. This provides the ability to process the analog data with highly accurate instantaneous speed and shaft position.
- Encoder adaptors that can use quadrature output to increase resolution or can be divided to reduce the output pulses. They also have LEDs that indicate a high on the index channel (once per rev) to facilitate setting engine TDC.
- Laser tachometers that use lined tape on rotating shafts to create an encoder in hard to reach places.
- A trigger board that automatically starts recording on the index channel (or other TTL input) under a variety of conditions.
- 400kHz analog channel that allows a sufficient sampling rate for high-speed valvetrain dynamics including all types of motor-sports valvetrains.

Some of the RAS software features used were:

- 2D, 3D and waterfall plots: time, speed or angular position with dynamic manipulation.
- Scaling: Data scaling on the scales x, y and z-axis.
- Statistics: maximum, minimum, average, etc.
- Combinations: combines individual measurements into one curve, i.e. 50-cycle average of average torque per revolution at a variety of speeds.
- Diagrams: saves analysis for future reference.
- Dissect Diagram: saves curve data for new diagrams
- Table to curve: imports table data, i.e. data for theoretical comparisons.
- Curve to table: export data to a table, i.e. Excel.
- Data reduction: reduces the angular position and analog data, i.e. export to Excel for theoretical comparison.

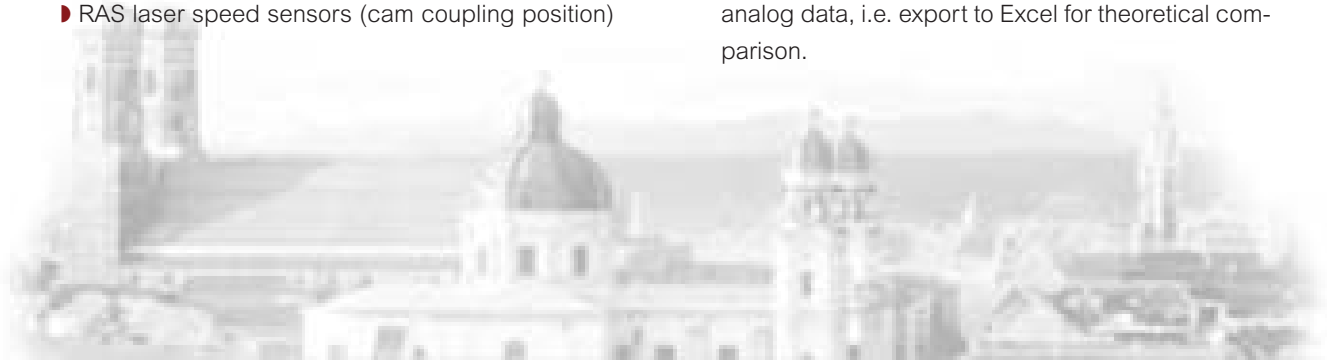

- Pitch correction: to remove discontinuities in laser tachometer lined tape encoders and gear tooth pitch errors.

Test Parameters

The test parameters for each cylinder head are described below.

VVL Cylinder Head

Speed control for each measurement consisted of:

- Speed run-ups: speed continuously increasing
- Speed steps: 250rpm steps to max speed
- Steady state: speed held constant

Temperature: ambient
Oil pressure: 52psi
Valve measured: Chamber three, primary valve and select others.

Ford V6 Cylinder Head

Speed control for each measurement similar to the VVL, except it started at 250rpm for the speed run-ups.
Temperature: 185°F
Oil pressure: 32psi (also 20 and 50psi)
Valve measured: Chamber six secondary valve

Measurements

The following data was collected for both cylinder heads (see Figure 1 for speed pickup locations):

- Valve lift
- Cylinder head movement
- Valve velocity
- Cylinder head velocity
- Cam torque

The following additional data was collected only from the VVL head:

- Valve Lift at max, 6, 3, 1.5, 0.5mm and min
- Cam speed
- Cam coupling end speed (laser tach)
- Torque sensor coupling end speed (laser tach)
- Torque sensor input speed (speed output)
- Flywheel speed
- Variable valve lift control shaft position
- Rocker strain
- Intermediate lever strain

The following additional data was collected only from the V6 head:

- Motor speed
- Cam coupling speed
- Torque sensor input speed

Analysis

This analysis is an assembly of select RAS Diagrams (plots) created from over 500 individual measurements and over 200 plots from the VVL and V6 cylinder heads. All of the testing, analysis and plots for each of the cylinder heads were completed in less than two weeks. It should be noted that any one (or many) of the more than 200 RAS plots could be looked at seconds after running the test, to verify test success and to modify test parameters and test plans from the information learned. The all VVL measurements and analysis were made at six fixed peak valve lifts (max, 6, 3, 1.5, 0.5mm and min) and with manually controlled valve lift sweeps. The V6 testing was done at a different test facility, requiring additional time to move and set up equipment. The testing was intended to characterize dynamics effects of two types of valve springs.

Speed

With the RAS's near real-time capabilities and using a speed run-up test, a new method is now available to view a continuous range of speeds and see what is happening between the typically measured fixed speeds and under dynamic conditions immediately after testing. Figure 4 shows a speed run-up and Figure 5 shows a stepped speed profile that was used, along with the typical constant speed data sets. The continuously stepped test was used to obtain valve lift, velocity, acceleration and torque signatures for comparison to theoretical models.

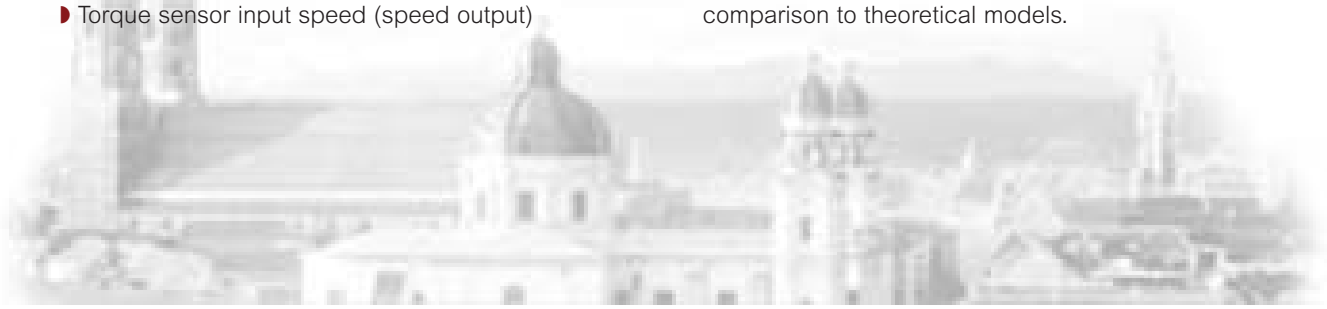

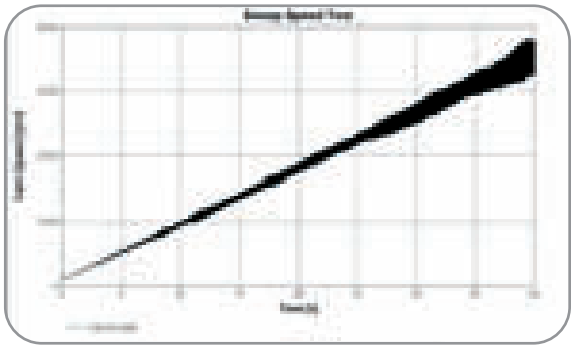

Figure 4 *0-3500rpm speed run-up (3750 for the V6)*

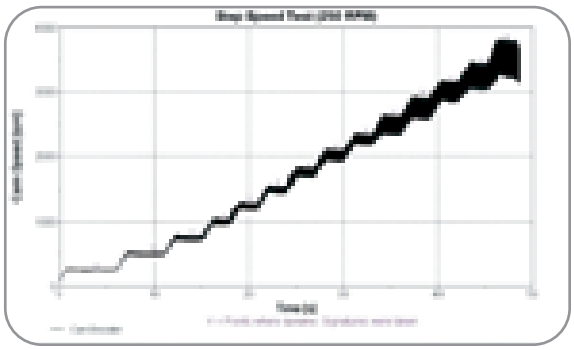

Figure 5 *250rpm speed steps to 3500*

Valve Lift, Timing and Head Displacement

Figure 6 shows a V6 valve lift waterfall plot with cam angle on the x-axis, cam speed on y-axis, and valve lift on the z-axis. This shows significant lift variation just below the peak test speed of 3750rpm.

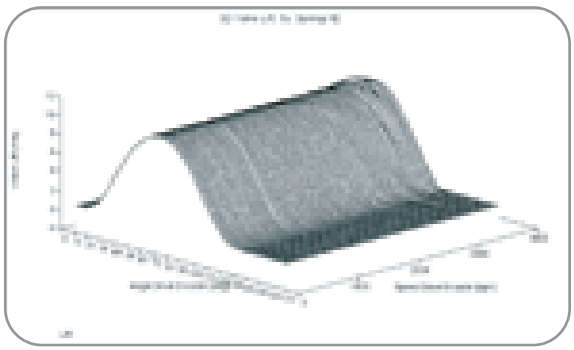

Figure 6 *V6 lift through a speed run up to 3750rpm*

Figures 7, 8 and 9 are V6 closing lift below 0.6 mm. Figure 7 and 8 are looking down the speed axis. Figure 8 is with 20psi oil pressure and Figure 9 is with 50psi. These show that the higher pressure in the lash adjuster adds extra load to the valvetrain and nearly doubles the valve closing motion to 0.15mm.

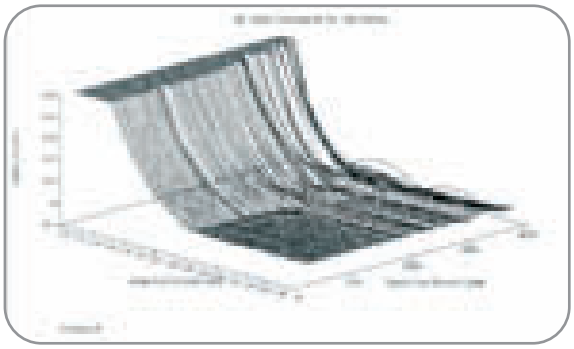

Figure 7 *V6 valve-closing lift under 0.6mm*

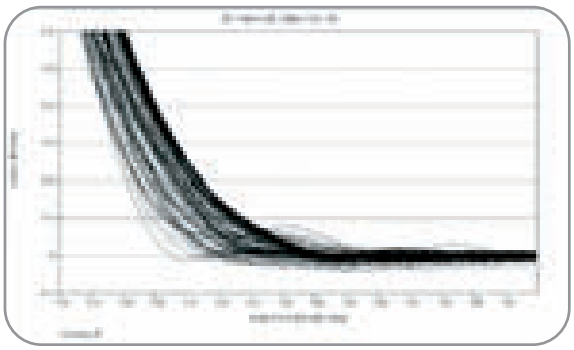

Figure 8 *V6 closing lift looking down the speed axis with 20psi oil pressure*

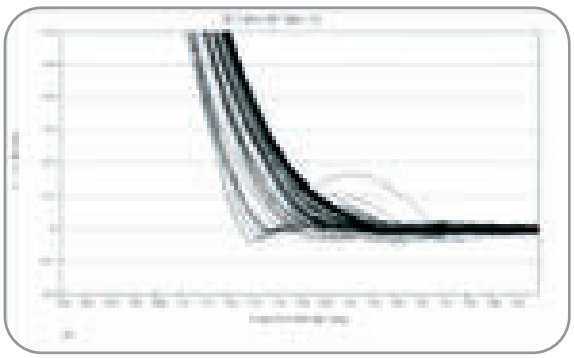

Figure 9 *V6 closing lift looking down the speed axis with 50psi oil pressure*

Figure 10 shows during a small speed change (3300-3400rpm) peak valve lift can vary up to 12 cam degrees. Figures 11 and 12 are from a new RAS valvetrain analysis tool. Figure 11 shows a sudden variation of 0.35mm in peak lift and 12 degrees in peak lift duration at 3300rpm and again at 3600rpm. Figure 12 shows a variation in opening and closing angles from 3400 to 3600rpm resulting in duration changes of plus two then minus seven degrees.

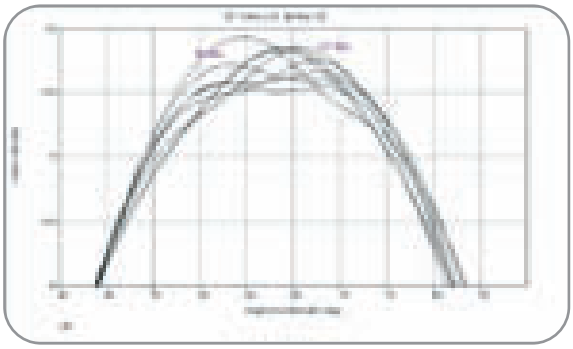

Figure 10 *V6 peak valve lift angular shift 3300-3400rpm*

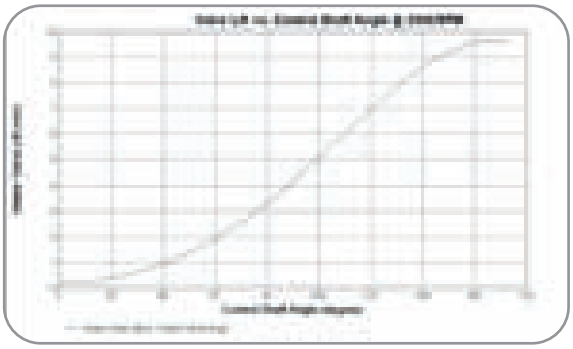

Figure 13 *VVL control shaft angle vs. lift*

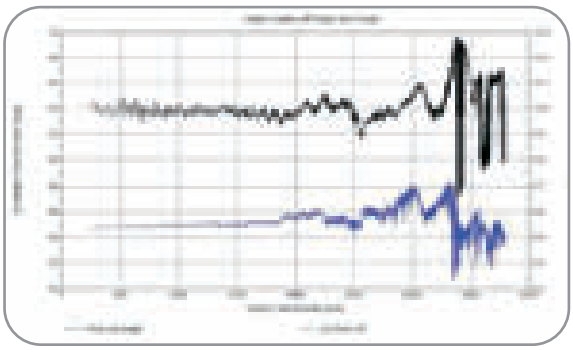

Figure 11 *V6 peak valve lift and angle*

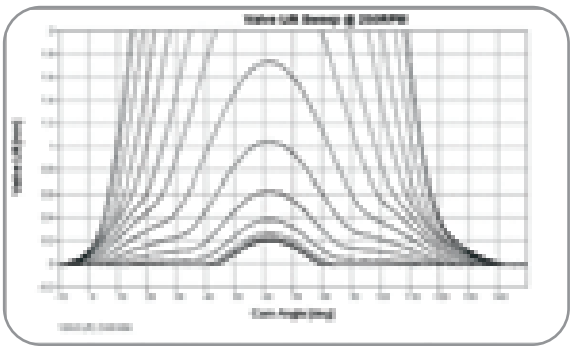

Figure 14 *VVL 0-2mm waterfall plot of varying lift*

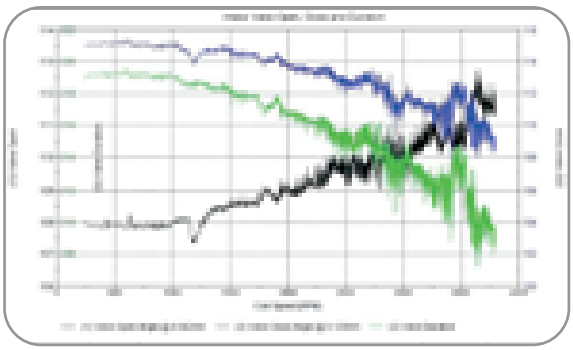

Figure 12 *V6 valve opening, closing angle and duration*

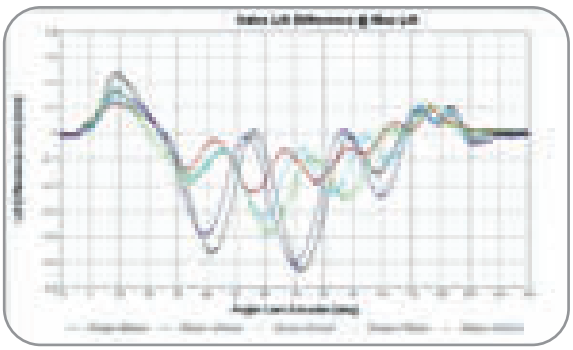

Figure 15 *VVL valve lift differences*

Figures 13 through 16 are from the VVL cylinder head, and demonstrate the flexibility of the RAS to perform more complex analyses on a variable lift valvetrain. Figure 13 is a plot of control shaft angle vs. lift. Figure 14 is a waterfall plot of varying lift, showing the long duration low lift (<2mm) characteristics of the VVL system. Both were easily created from one manually controlled 10-second lift sweep at 250rpm. Figure 15 is a plot of the near kinematic valvetrain lift at 250rpm, with lift at speeds from 2500 to 3500rpm

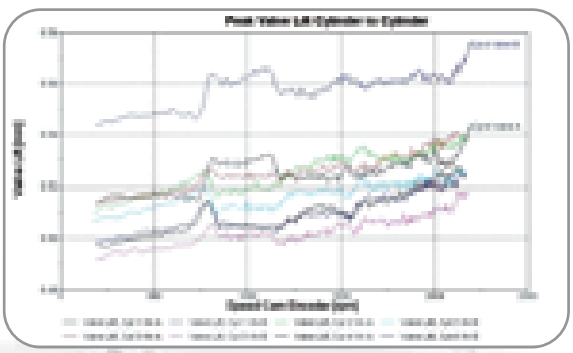

Figure 16 *VVL combined valve lift plot*

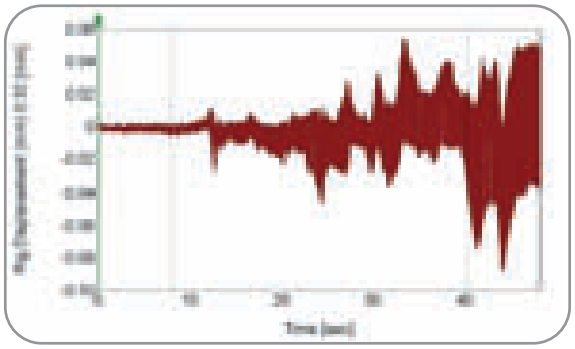

Figure 17 *V6 raw data plot of cylinder head movement*

subtracted. The analysis shows up to 0.8mm valve-train deflection at higher speeds. Figure 16 is a peak valve lift per revolution curve overlay of all eight VVL valves, measured during eight separate speed run-ups (figure 4).

Figure 17 is a raw data .bmp showing the amount of V6 cylinder head motion as measured by the HSV's optional external displacement decoder. The VVL head was similar.

Valve Velocity

Figure 18 is a V6 waterfall plot of valve velocity from 250 to 3750rpm. Figure 19 is a close-up of Figure 18 looking down the speed axis at valve closing. This

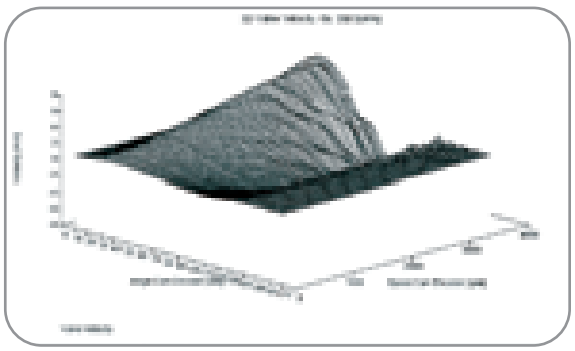

Figure 18 *VVL valve velocity waterfall plot*

portion of valve event has been of particular interest recently, with many companies writing special code to evaluate valve-closing velocity. This is commonly done with proximity probes that only measure valve motion about 1mm from the valve seat.

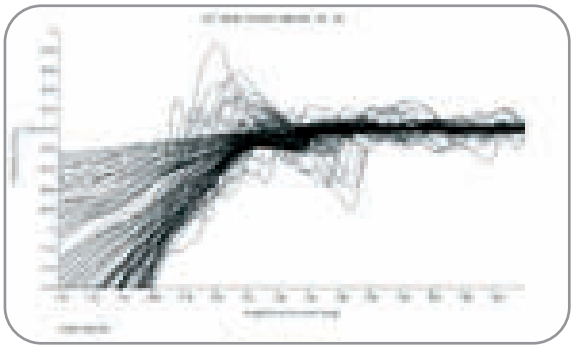

Figure 19 *Valve closing velocity close-up*

Figure 20 is the new evaluation for valve closing velocity at 0.05 and 0.15mm of lift from the V6 head. This type of evaluation may be of interest prior to actual valve closing, but much more valuable information is available in the following valve acceleration analysis.

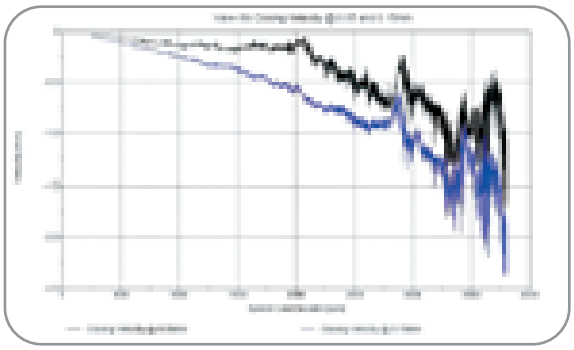

Figure 20 *V6 valve closing velocity on a speed run-up*

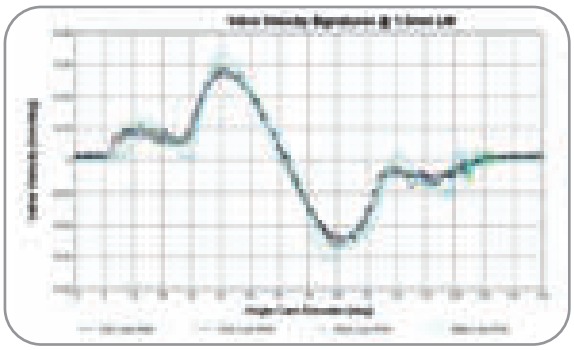

Figure 21 *VVL normalized valve velocity mm/deg*

Figure 21 shows a normalized valve velocity signature plot (mm/deg) of the VVL at 1.5mm of valve lift at 500, 1500, 2500 and 3500rpm

Valve Acceleration

Figure 22 shows a V6 valve acceleration waterfall plot. This acceleration information is more directly related to valve loads than valve closing velocity measurements. This is because valve loads are not at their peak at the near valve closing points where velocity is currently being measured. Valve load is much higher at the point of valve seating and valve separation. Figure 23 is looking down the speed axis of Figure 22 and shows the cam lobe zones that are defined for the peak acceleration analysis of Figure 24. Figure 24 contains the maximum opening, minimum nose, maximum closing and minimum and maximum seating accelerations of the valve for a speed run-up (figure 4.) Figure 25 is the same analysis as Figure 24 but is a combination of a large number of fixed speed data sets. These data sets contain 50 revolutions and the curve data points are an average of the 50 peak values. The speed run-up took 46 seconds to record; the fixed speed test took several hours. Figure 26 is a plot of measured VVL valve lift, velocity and acceleration, and cam torque. These 3500rpm measurement signature curves can be overlaid with imported theoretical model data for comparison. This plots acceleration was calculated using a 5kHz filter on velocity.

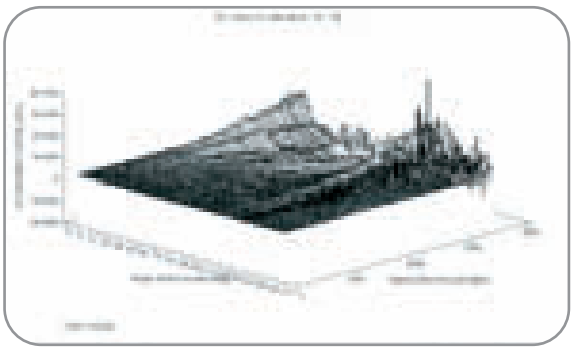

Figure 22 *V6 valve acceleration waterfall plot*

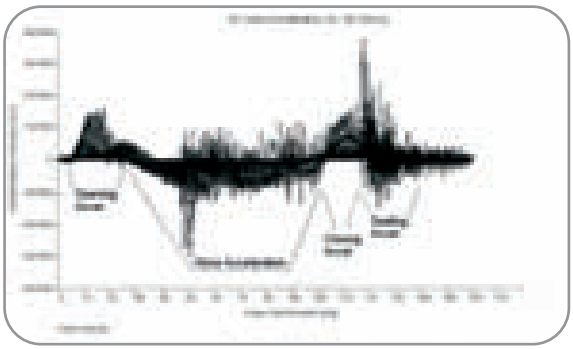

Figure 23 *V6 valve acceleration looking down the speed axis; valve opening, nose, closing and seating.*

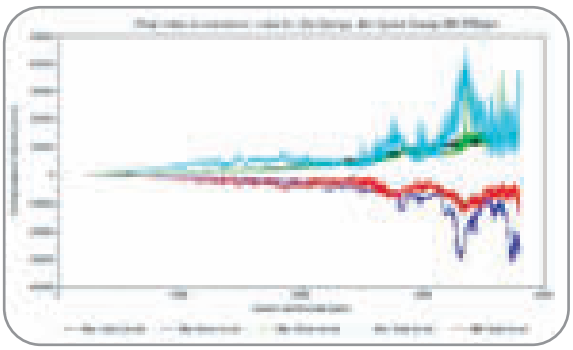

Figure 24 *V6 peak valve accelerations (run-up)*

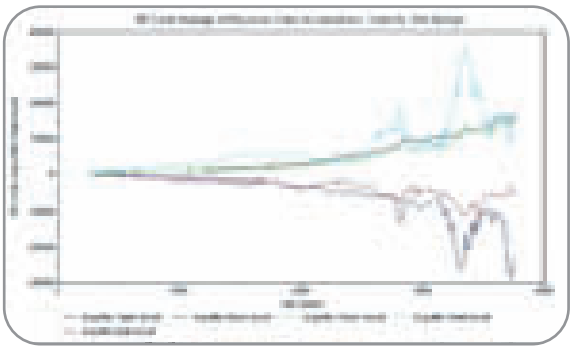

Figure 25 *V6 peak valve accelerations (avg)*

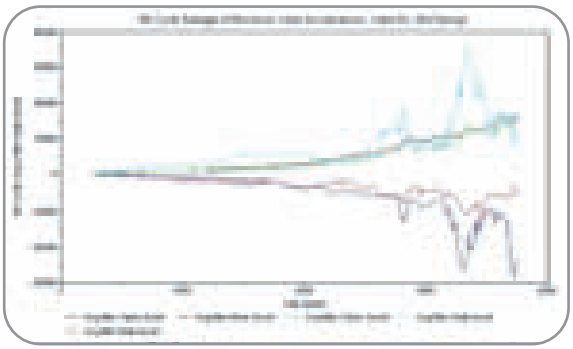

Figure 26 *V6 measured valve lift, velocity and acceleration at 3000rpm with theoretical data.*

Cam Torque and Power

Selection of the correct torque sensor is important to the results of friction torque and torque signatures. Table 1 shows the VVL bench test system frequency with different torque sensors. Figures 27-29 are from the VVL and demonstrate the effect of torque sensor stiffness on peak torque per revolution of the test. Figure 27 is a 1604-200inlb torque-sensor with stiffness low enough to create a 160Hz system frequency. At 2400rpm vibrations were so severe the test had to be terminated. Figure 30 is a waterfall plot of the 1604-200.

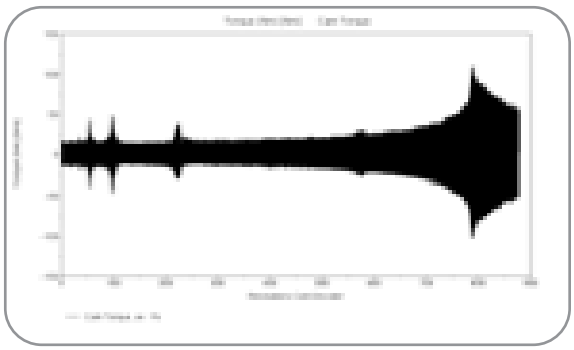

Figure 27 *1604-200inlb torque sensor*

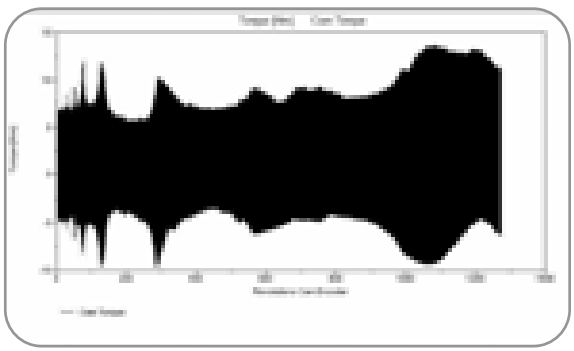

Figure 28 *1104-500inlb torque sensor*

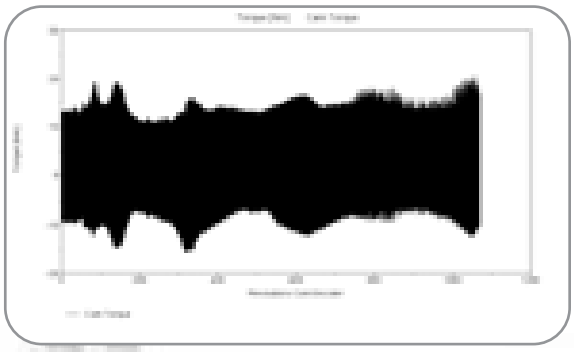

Figure 29 *1604-1000inlb torque sensor*

Lebow Torque Sensor	*Max Torque (lb in)*	*Stiffness (Nm/rad)*	*System frequency (Hz)*	*Resonant speed (rpm)*
1604-200	*200*	*3728*	*160*	*2400*
1105-500	*500*	*5100*	*185*	*2700*
1604-1000	*1000*	*16000*	*255*	*3850*
1604-500	*500*	*9603*	*228*	*3420*

Table 1: Torque sensor, system frequency and speed

A Himmelstein MCRT 49060V(5-2)CNXLK flange mount torque sensor was selected for all future testing. It has a stiffness of 68,000Nm/rad, 10v output, 1100Hz frequency range and higher accuracy. To increase stiffness and minimize torsional vibrations it will be attached to the flywheel reducing the number of couplings to one and a one inch or larger shaft will be used to drive the camshaft. For non-torque related measurements testing can be done with a steel spool in place of the torque sensor to further stiffen the system and reduce vibrations.

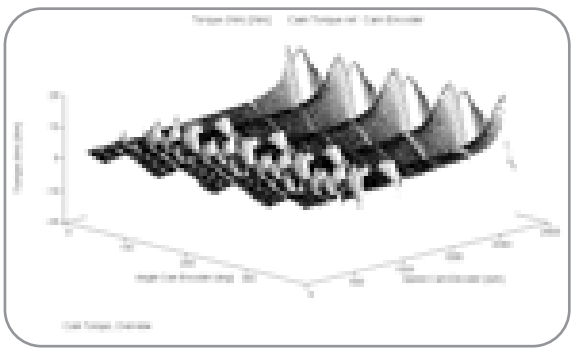

Figure 30 *1604-200inlb torque sensor*

Figures 31-32 demonstrate how different system frequencies affect torque signatures. Speeds of 500, 1000, 1500 and 2000rpm are shown. Figure 33 is a comparison of friction torque (average per revolution) from the different sensors during speed run-ups (Figure 4). The 1604-200 and 1104-500 exhibit visible effects on the measurement calculation.

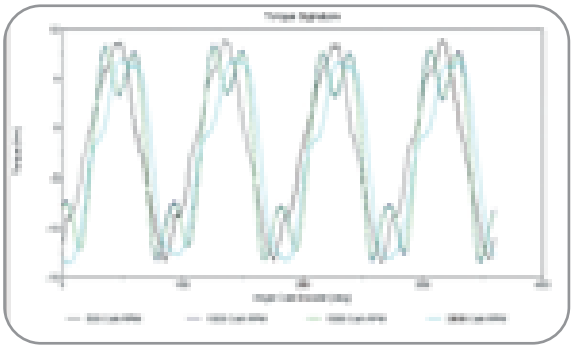

Figure 31 *1105-500inlb torque signatures*

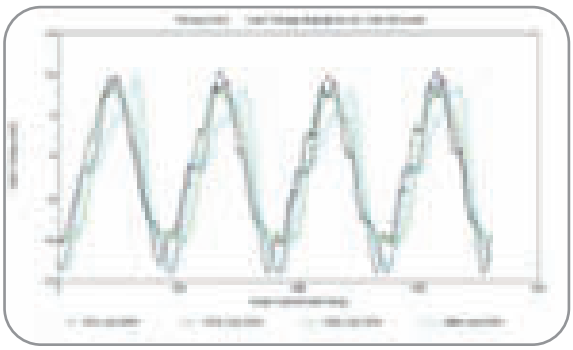

Figure 32 *1604-1000inlb torque signatures*

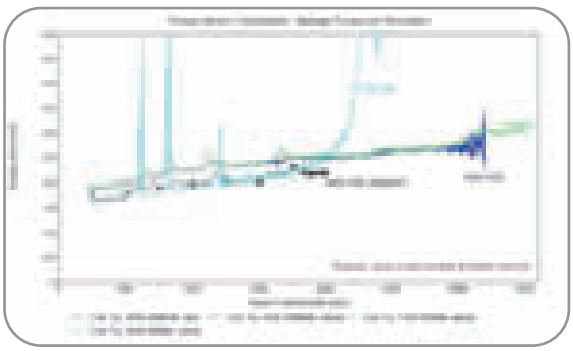

Figure 33 *VVL friction torque and sensor comparison*

Figures 34-35 are frequency and order spectrums from the 1604-200 torque sensor. Figure 34 shows the 160Hz system frequency that the 1604-200 torque sensor causes. Figure 35 show the 160 Hz drive system frequency crossing multiples of the fourth order of speed and the corresponding speed amplitude variation.

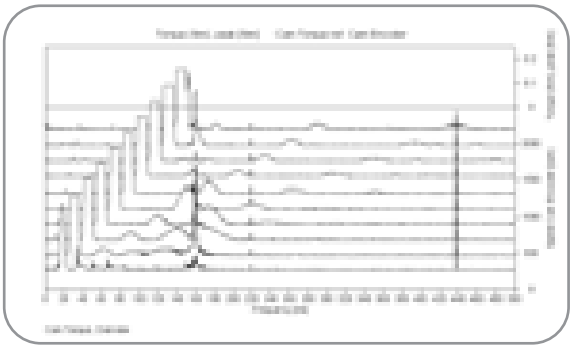

Figure 34 *1604-200 torque frequency spectrum*

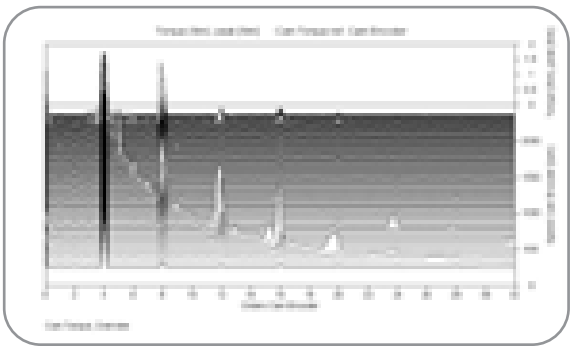

Figure 35 *1604-200 torque order spectrum*

Power and Friction Torque

Figure 36 shows the relationship between friction torque and power with the 1604-200 torque sensor.

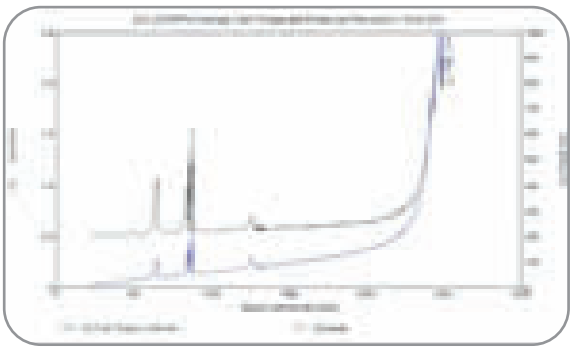

Figure 36 *1604-200 friction torque and power*

Torsional Vibration

The unique capabilities of the RAS's speed channels and software simplify analysis of torsional vibrations.

As shown in Figure 1, four speed channels were used to determine the amplitude of the vibrations. Figure 37 shows that the majority of the peak vibration was attributable to the 1604-200 torque sensor. Table 2 shows the peak vibration angles for various torque sensors used on the VVL head. Effect of the vibrations on data can be seen in Figures 30, 31 and 32.

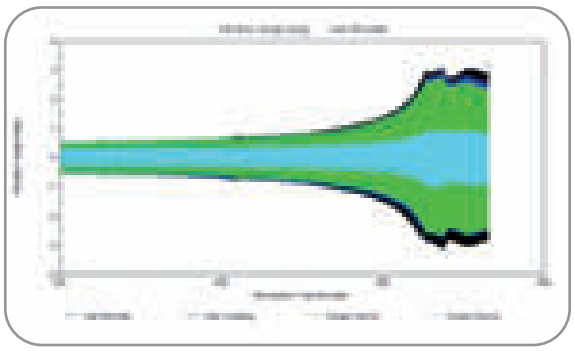

Figure 37 *1604-200 vibration angles at four drive points*

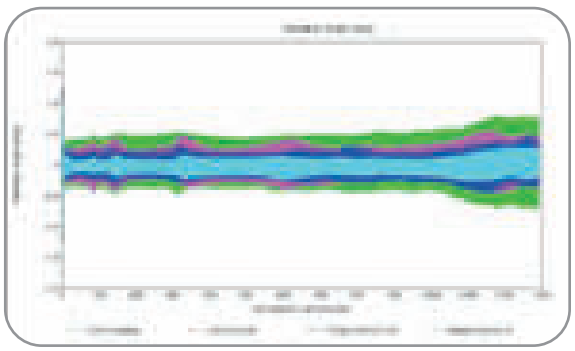

Figure 38 *1604-1000 vibration angles at four drive points*

Lebow Torque Sensor	*Max Torque (lb in)*	*Stiffness (Nm/rad)*	*Max System Vibration (degrees)*
1604-200	*200*	*3927*	*± 3.5°*
1105-500	*500*	*5100*	*±0.75° (±2° Ford V6)*
1604-1000	*1000*	*16000*	*±0.5°*
1604-500	*500*	*9603*	*±0.5°*

Table 2: Vibration angle for different torque sensors

Figure 39 is a V6 cam coupling vibration angle waterfall plot looking down the speed axis during a speed run-up. This shows almost two degrees of vibration at higher speeds. Since the encoder on this test cell was mounted to the high inertia drive motor, a laser tachometer had to be mounted at the cam coupling to measure this vibration. This two-degree vibration can also be seen in the lift data at the top of Figures 7-9 and demonstrates the need to have an encoder mounted directly to the camshaft and to have a stiff drive system. A 1104-500 torque sensor was used here.

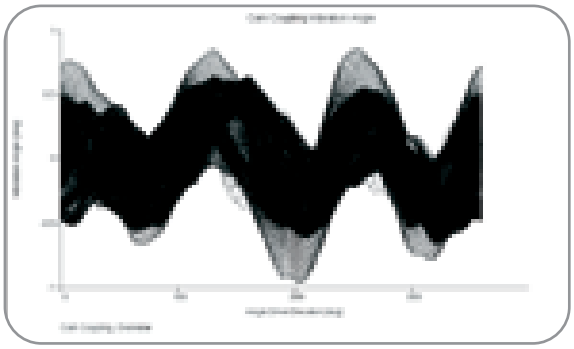

Figure 39 *V6 cam coupling vibration*

Figure 40 *RAS torsional model*

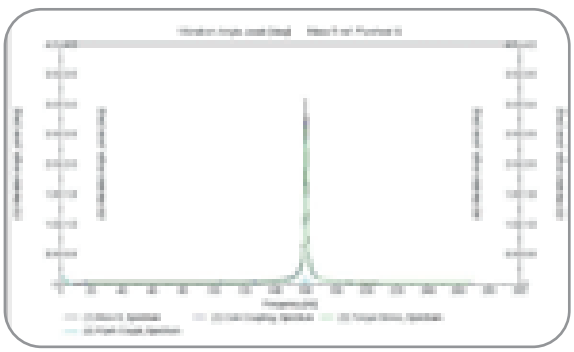

Figure 41 *RAS torsional model frequency/angle results*

Figures 40-41 show the RAS's torsional model and frequency results used to predict the system response with the 1604-200 torque sensor.

Rocker arm strain

Figure 42 shows VVL Roller Finger Follower (RFF) strain over a speed run-up. The point marked with a "V" is where the rocker arm strain is equal to base circle strain indicating that valetrain separation may be imminent or occurring. This measurement was repeated with peak valve lift set at max, 6, 3, 1.5, 0.5mm. Figure 43 is a plot of these points split into three areas; low opening lift, major lift and low closing lift.

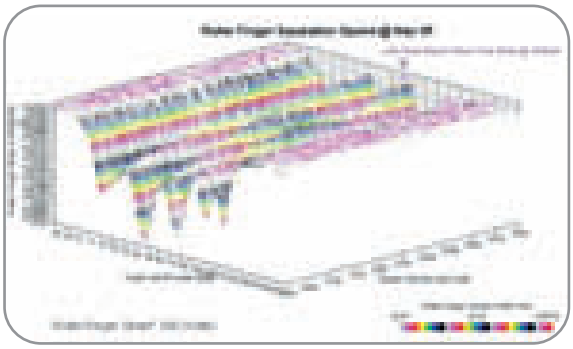

Figure 42 *VVL RFF strain during a speed run-up*

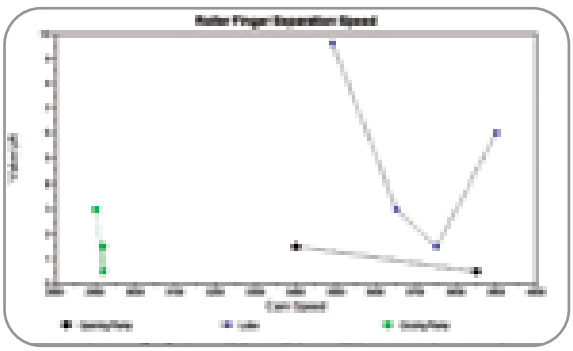

Figure 43 *VVL RFF separation speed for various lifts*

Filtering and Sample Rate

No hardware filtering was used on any measurements in this paper. A Butterworth digital 8th order filter was used on velocity signals to calculate acceleration. Up to this point (except as indicated), 5kHz filter frequency was used for acceleration signatures and a 15kHz frequency for all other acceleration curves. Figure 44 shows the effect of 10, 15, and 20kHz filter frequencies on acceleration calculations. This shows that acceleration amplitude is continuously increasing with filter frequency, indicating dampening of the acceleration signal during closing. With the following exception, the sample rates used for lift and velocity were 200ks/s.

Figure 45 shows the effect of valve velocity sample rate (50, 100, 200 and 400ks/s) and filter frequency (15, 20, 50 and 100kHz, respectively) on the valve seating portion of acceleration at 3750rpm. The velocity curve (upper set) includes a raw 400ks/s unfiltered measurement and has the steepest slope. The change in slope of the other curves is due to the sample rate and filtering. The calculated acceleration (lower curve set) demonstrates the need for high filter frequencies and acquisition rates to quantify valve-seating acceleration.

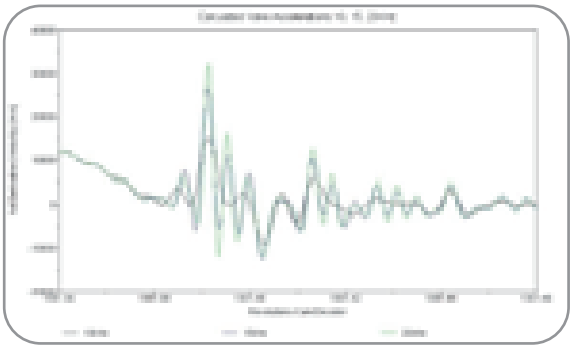

Figure 44 *Acceleration with 10, 15 and 20kHz filters*

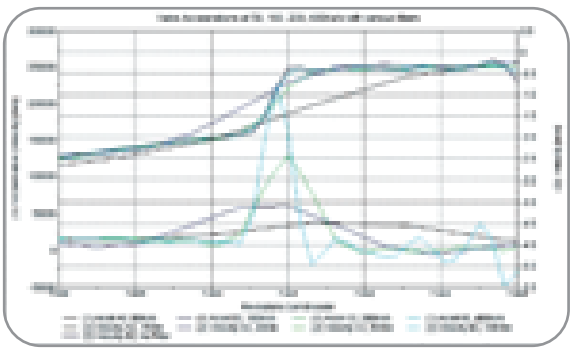

Figure 45 *Effect of various valve velocity sample rates and filter frequencies on closing acceleration*

Conclusion

The analysis section clearly shows that a magnitude higher level of information about valvetrain dynamics can be obtained when the Rotec RAS's near real-time analysis capabilities, in combination with the Polytec PI HSV's ability to provide full valve motion, are used. The RAS's 400kHz analog channels and the high bandwidth (50kHz-Velocity and 250kHz-lift) of the HSV provide more complete information about valve dynamics than was previously available, and were operated on other engines to speeds in excess of 9,000 and 15,000rpm.

The RAS's near real-time analysis capabilities also allow immediate adjustment of test parameters and test plans during testing. In addition to providing 40-bit camshaft position, the RAS's speed channels quickly identified bad drive motor bearings, a defective optical encoder and drive speed control issues during testing.

Also shown is the requirement of a stiff torque sensor and drive system for accurate toque measurements and that speed run-ups provide a method to reduce the number of test data sets and further simplify valvetrain dynamics testing. This combination of state-of-the-art equipment provides unique and more complete insight into valvetrain dynamics and provides methods to significantly reduce test and analysis time.

References

[1] Andreas R. Schamel, Joachim Hammacher, and Dietrich Utsch, Ford Motor Co., Modeling and Measurement Techniques for Valve Spring Dymanics in High Revving Internal Combustion Engines SAE 930615

[2] In-Soo Suh, Daewoo Motor Co., Richard H. Lyon, RH Lyon Corp, An Investigation of Valve Train Noise for the Sound Quality of I. C. Engines, SAE 1999-01-1711

[3] J. W. David, North Carolina State University, Dojoong Kim, Ulsan University, J.A. Covey, General Motors, Optimal Design of High Speed Valvetrain Systems, SAE 942502

[4] Ronald L. Stene, James Westbrook III and David Eovaldi, Chrysler Corporation, Analyzing Vibrations in an Internal Combustion Engine, SAE 980570

New Equipment and Methodology to Perform High Speed Valvetrain Dynamics.
Jeff G. Sczepanski, Ford Motor Company, Dearborn, USA.
From SAE World Congress, Detroit 2004.
SAE Paper No. 2004-01-1720

Improved Approaches to the Measurement and Analysis of Torsional Vibration

Seán Adamson, Rotec GmbH, Munich

Abstract

A primary goal of NVH engineering is the identification and control of noise and vibration sources. In recent years the torsional vibration behaviour of engine and powertrain components has gained in significance. This paper discusses several aspects of measuring and analysing torsional vibration and related data. Several torsional vibration measurement techniques are presented, together with remarks on precautions against possible sources of error, and the order of accuracy to be expected of the test results. Two applications requiring multichannel measurement and analysis are outlined.

Introduction

Understanding and controlling torsional vibration is of profound importance in vehicle development, refinement and optimisation. The primary source of torsional vibration is the internal combustion engine. Periodic combustion impulses result in rotational speed fluctuations of the crankshaft. Ignition and combustion within a cylinder cause a rapid rise in gas pressure and an angular acceleration of the crankshaft. Gas compression in the next cylinder causes immediate deceleration. Torque pulsations result in crankshaft torsional vibrations which reach the camshaft(s) and auxiliaries via belt or chain drives. In addition, the torsional vibrations which enter the gearbox may be transmitted further via propeller shafts and differentials to the vehicle wheels [1, 2, 3].

Increasing demands to shorten development cycles mean that less time is available for both testing and mathematical modelling. Meaningful solutions may not be arrived at by treating vibration dampers, timing belts, gear stages, etc. as isolated components. Comprehensive studies of the complete system are required which take interactions between individual components into account. Rotec GmbH was formed in 1988 to develop portable, PC-based equipment for use in torsional vibration testing. The company places high emphasis on accurate acquisition of torsional vibration data and the primary analysis methods are based on the revolution domain as opposed

to the time domain. In recent years the company has exploited both the increased computational power of PCs and digital signal processing technology to help make multichannel measurement and analysis quicker and more effective. This paper begins by presenting the new generation of ROTEC-RAS equipment (RAS = Rotation Analysis System). Torsional vibration measurement methods are then reviewed. Sources of error are highlighted and the degree of accuracy of test results is discussed. Two applications in engine and powertrain testing are utilised to illustrate the capabilities of the equipment.

The New Range of RAS Equipment

Applications requiring multichannel torsional vibration measurement include optimising engine timing and auxiliary drive systems, tuning of vibration dampers, minimising clutch slip, reducing gearbox rattle and transmission error testing of gearsets. This type of testing may also require additional measurement of transverse vibrations synchronous to the rotational data [4, 5]. All RAS channels operate on a common time-base making accurate, phase-matched, cross-channel analyses possible (e.g. accurate calculation of the angular displacement between two rotating shafts). The RAS rotational speed channels require square-wave TTL level signals as input. The time interval between rising (or falling) edges for each pulse period is measured using a high-speed counter/timer (10GHz/40-bit). Input of index pulse and rotational direction signals is also provided for. The RAS analogue channels sample at either 50kHz or 400kHz with 16-bit resolution. Digital downsampling, anti-aliasing protection, programmable gain, AC/DC coupling and differential or ICP inputs are provided. By making use of a commercially available interface board, Controller Area Network (CAN) signals may be directly input and analysed in a similar way to analogue signals. CAN information is increasing in relevance since this is the dominating serial bus system for in-vehicle networks of passenger cars, as well as trucks and buses. RAS systems are modular (both hardware and software), scalable to fit operational needs and used both in test cell and in-vehicle applications. Figure 1 summarises NVH signal types and sources.

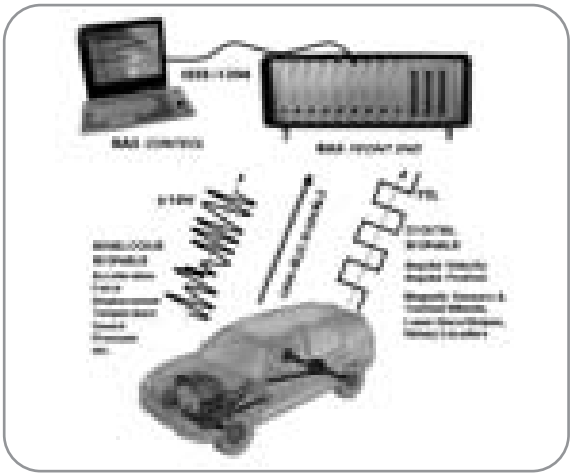

Figure 1 *Test Vehicle, Signals and RAS System*

Angular Velocity Measuring Methods

The digital measurement technique for torsional vibration is based on sampling at equidistant angular intervals around the rotating shaft. This is generally accomplished by one of three methods: (i) mounting an incremental rotary encoder onto the shaft, (ii) scanning a toothed wheel with a magnetic pickup, (iii) targeting reflective/non-reflective (black/white) bar patterns with an optical sensor. The sensor electronics generate an angular velocity signal in the form of a TTL pulse train. The frequency of the pulse train is directly proportional to the angular velocity of the shaft. Rotary encoders with high line counts, as used in single flank testing of gearsets, can provide thousands of pulses per revolution, whereas proximity sensors are limited to a maximum of several hundred pulses per revolution.

Angular sampling provides a fixed number of samples per revolution and is independent of the rota-

tional speed. When time sampling is used, the number of measure-ment values per revolution varies with rotational speed. A primary advantage of revolution domain analysis is the elimination of leakage errors from spectral components that are order related. Assuming that the angular velocity is constant between adjacent pulses, the instantaneous angular velocity values may be calculated by dividing the actual angular spacing of the physical steps (between gear teeth or encoder lines) by the elapsed time from one positive edge to the next (T_1, T_2, T_3, …) as shown in Figure 2.

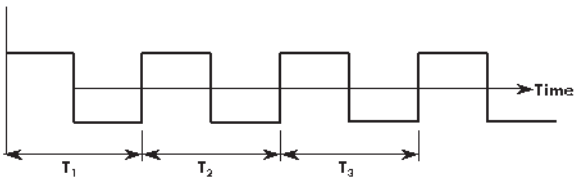

Figure 2 *Standard Rotational-Speed Pulse Train*

Figure 2: Standard Rotational-Speed Pulse Train
The RAS counter/timer frequency of 10GHz per channel (corresponding to a 100ps time base) results in an extremely high angular resolution, $\Delta\theta$, which is given by

$$\Delta\theta = \omega \times 10^{-10} \quad (1)$$

with the angular velocity, w, in degrees/sec and $\Delta\theta$ in degrees. For example, the angular velocity of a shaft rotating at 2400 rpm (40Hz) is 7200 deg/s corresponding to an angular resolution of 1.44 µdeg.

Sources of Error in Angular Velocity Measurements

There are three main causes of innaccuracies in angular velocity measurements:

1. Errors in measuring pulse train periodic times
2. Errors due to sensor vibration or relative movement between proximity sensor and target
3. Errors due to variations in tooth spacing

Measuring Pulse Train Periods

A high number of clock counts per pulse period allows measurement of pulse train periods with an accuracy of ±1 count (quantisation error, assuming no clock jitter). Even for encoders with high line counts rotating at high speeds, the RAS 10GHz speed-channel clock ensures a high number of 100psec increments between adjacent pulse train edges. Consider an encoder with 4500 lines rotating at 6000rpm. The pulse frequency is 450kHz (period = 2.2×10^{-6}s) and the number of increments per period is

(10GHz / 450kHz) = 2.5×10^5 counter increments

This corresponds to a percentage error of 4×10^{-6}% and may therefore be neglected. Indeed, the RAS angular resolution – of the order of milli arc seconds at typical rotational speeds – greatly exceeds the measuring uncertainty of even the best rotary encoders available today which are specified to several seconds of arc. Since the RAS time resolution vastly exceeds the accuracy of all angular velocity sensor arrangements, the error associated with measuring pulse train periods is negligible.

Sensor Movement

Vibration of the proximity sensor in a direction parallel to the target teeth or reflecting pattern produces a signal that is indistinguishable from angular velocity fluctuations. This error can be eliminated by making the sensor mount stiff enough so that sensor vibration is above any angular velocity signal of interest.
Relative movement between the target and the proximity sensor during a measurement can have two main causes: The target may move nearer to or further away from the sensor when the shaft is subjected to particular loads. Compared to the normal state, the sensor will encounter a tooth/reflecting marking either too soon or too late and this results in incorrect angular velocity values. A second cause is when toothed wheels or optical targets are mounted eccentrically. A 1st order signal is produced which can-

not be distinguished from a genuine 1st order produced by machine vibrations. In order to distinguish between first order machine problems and 1st order imbalance two sensors can be positioned 180 degrees radially opposite to one another. By taking the average value of the two angular velocity signals, the 1st order signal components produced by eccentricity are eliminated.

Tooth Spacing Variation

All toothed wheels and gears have some degree of variation in tooth spacing. A toothed wheel and magnetic sensor arrangement will generally provide less accurate angular velocity measurement results than a shaft encoder. This section gives an outline of how measurement errors caused by tooth spacing inaccuracy may be quantified.

A rotational speed adapter was machined in the workshop. It comprises an inner toothed wheel with 72 teeth which can be directly coupled to the rotating shaft and a magnetoresistive sensor fitted into an outer bracket which does not rotate. The sensing gap was fixed at 1mm. A calibration measurement over many revolutions was performed by rotating the adapter on a lathe (with minimal speed fluctuation). The sensor signal was input to a RAS speed channel for analysis. Figure 3 clearly shows that the noise pattern in the angular velocity signal primarily caused by tooth spacing variation errors repeats every revolution. Figure 4 shows the actual pitch error from tooth to tooth averaged over many revolutions. Both the individual tooth-to-tooth error and the cumulative error are shown. The cumulative error curve displays a first order inherent in the adapter thought to be caused by the machining process on the milling machine.

Once the pattern caused by tooth spacing error has been identified, the data are saved and used to analytically remove the error from subsequent measurements.

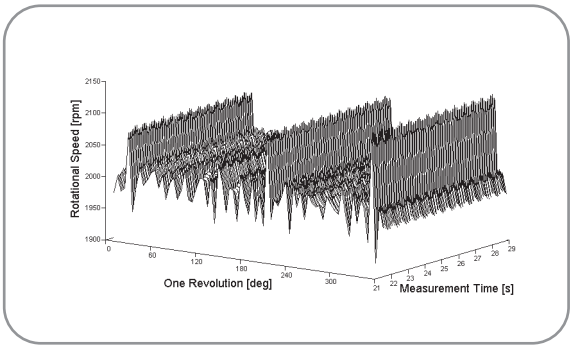

Figure 3 *Pattern of Tooth Spacing Variation*

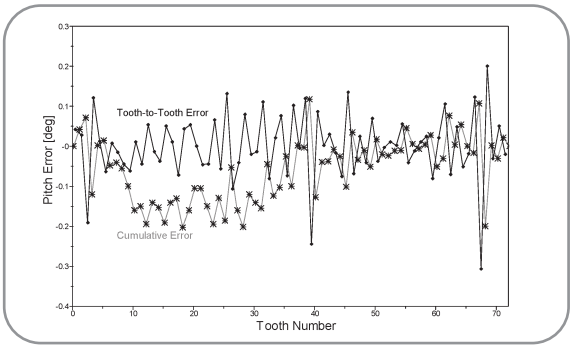

Figure 4 *Tooth-to-Tooth Spacing Errors*

Figure 5 shows data from a speed ramp measurement on a 4-cylinder engine using the toothed-wheel adapter bolted onto the front end of the crankshaft. The grey curve represents the raw time history data. The black curve results when the data of Figure 4 are used to remove the tooth spacing error.

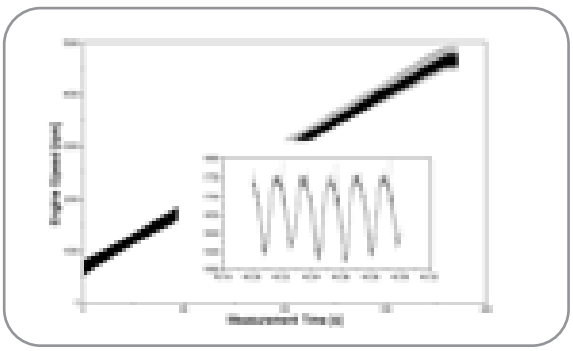

Figure 5 *Removal of Tooth Spacing Errors*

Errors in Spectral Analysis Arising from Indadequate Sampling Rates

Shannon's sampling theorem states that a signal may be detected up to half the sampling frequency (the Nyquist frequency). This value of half the sampling frequency is equal to the maximum value of frequency (or order) seen in the spectrum. (An order is a harmonic vibration whose period is an integer number of revolutions of a reference speed channel). The effect of 'aliasing' is to allow frequencies higher than the Nyquist frequency being reflected back into lower frequencies causing false indication of spectral lines. Care must be taken when trying to identify and deal with errors which may arise from undersampling in the time domain and aliasing in the spectral domain. The highest frequency components present in the signal must be known before a decision is made on a suitably high sampling rate.

With analogue signals it is possible to use a low-pass hardware filter before the signal is sampled in order to suppress frequency components which are too high for the sampling rate used. In addition, the signal may first be sampled at a high sampling rate and then digitally filtered to remove the higher frequency components before sampling again at a lower rate (both procedures are used with RAS analogue channels).

Compared to the sampling of analogue quantities (sampling rate, sample & hold circuit) counter/timer data acquistion channels record the time interval required for the test object to rotate through a finite angular interval as shown in Figure 6. Rather than measuring the instantaneous angular velocity, ϖ, at a given point on the shaft circumference, an average velocity, ϖ, for a finite angular interval, $\Delta\varphi$, between adjacent measurement points is measured. This causes a damping of the measured speed amplitudes which depends on both the number of measurement points per revolution, N, and the rotational harmonic order of interest, *i*.

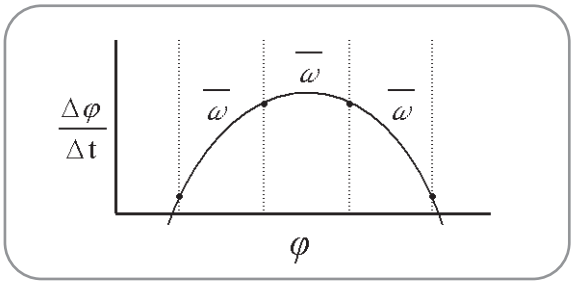

Figure 6 *Angular Velocity Curve with Angle-Equidistant Data Points (•)*

The rotational speed fluctuation for a single order is

$$\omega(\varphi) = A \cdot \cos(i \cdot \varphi) \quad (2)$$

Since a cosine signal has its maximum value, A, at $\varphi = 0$ and assuming that the measurement points are symmetric to $\varphi = 0$ at $-\Delta\varphi/2$ and $+\Delta\varphi/2$, then the average rotational speed in the interval $\Delta\varphi$ is:

$$\bar{\omega}(\varphi) = \frac{1}{\Delta\varphi} \cdot \int_{-\Delta\varphi/2}^{+\Delta\varphi/2} \omega(\varphi)\, d\varphi$$

$$= \frac{1}{\Delta\varphi} \cdot \int_{-\Delta\varphi/2}^{+\Delta\varphi/2} A \cdot \cos(i\varphi)\, d\varphi$$

$$= \frac{A}{i \cdot \Delta\varphi} \cdot \left[\sin\left(i \cdot \frac{+\Delta\varphi}{2} \right) - \sin\left(i \cdot \frac{-\Delta\varphi}{2} \right) \right]$$

$$= \frac{2 \cdot A}{i \cdot \Delta\varphi} \cdot \sin\left(i \cdot \frac{\Delta\varphi}{2} \right)$$

$$= A \cdot \frac{N}{i\pi} \cdot \sin\left(\frac{i\pi}{N} \right) \quad (3)$$

Equation (3) shows that the speed measured will always be lower than A, its maximum value.

For a given order, i, amplitude damping as a percentage is given by:

$$A(i)\ \% = 100\left[1 - \frac{N}{\Delta\pi}\sin\left(\frac{\Delta\pi}{N}\right)\right]$$

The ratio $i/N = 0.5$ gives the cut-off order according to sampling theory. Accuracy is best in the limiting case of the sampling interval approaching zero, i.e. an infinite number of measurement points! Four-stroke internal combustion engines produce excitation at multiples of half engine order up to 12th order angular velocity. Using a toothed wheel with 48 teeth would mean a 0.7% degree of damping in the calculated 2nd order amplitude but a greater degree of damping (10%) for order 12. By doubling the number of teeth to 96, a lesser degree of damping results for 12th order amplitude (now 3%).

Enhanced Resolution with Gear Tooth Sensors

Chain sprockets or gears within a gearbox possess a relatively low number of teeth. When such wheels have to be used as targets for proximity sensors, their low number of teeth prohibits FFT analysis to higher harmonics. In order to increase the amount of information per revolution obtained when using this type of wheel, a so-called 4-fold sensor has been developed. The sensor head contains four magnetoresistive elements and a permanent magnet. The sensor provides four times more information per revolution than standard speed sensors. Figure 7 shows the 4-fold pulse train.

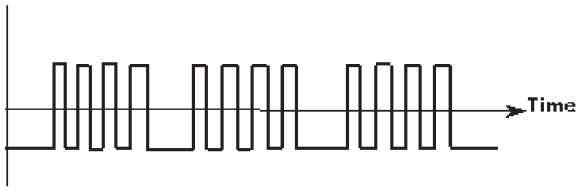

Figure 7 *Removal of Tooth Spacing Errors*

The 4-fold signal contains a repeating pattern of three short periods followed by a longer one. The three shorter periods represent the passing of a tooth; the longer period results from the next approaching tooth. A RAS software algorithm uniformly distributes the 4-fold sensor information in the revolution domain prior to time or spectral analysis. In order to obtain optimum results, the pitch of the toothed wheel should be similar to the separation of the individual magnetoresistors in the sensor head. This ensures that the longer period in the pulse trains does not dominate.

Fast Fourier Transform Analysis

RAS software allows for both frequency and order analysis of measurement data using the Fast Fourier Transform (FFT) method. Frequency spectra require input time domain data expressed as a function of time. Order spectra require input data expressed as a function of revolutions of a reference channel. For both frequency and order analysis the time history curve is sub-divided into records (analysis intervals) of equal length. The spectral resolution is the reciprocal of the size of the analysis interval. The FFT yields n/2 spectral lines for an interval size of n data points (each line has a real and an imaginery part).

A fundamental assumption of FFT analysis is that the signal contains only exact harmonics within the analysis interval. Furthermore, each harmonic component must start and stop at the same amplitude with the same slope, i.e. if the signal were immediately repeat-

ed it would be smooth and continuous. So-called leakage errors will arise if these conditions are not met.
For engine tests the width of the analysis intervals is usually set to 4 revolutions of the crankshaft (2 cycles of system excitation) which ensures that only exact harmonics are contained within each interval. Care needs to be taken, however, when analysing powertrain data. Transmitted engine vibrations retain their frequency but their amplitude and order will vary with transmission ratios. When order analysis is to be performed at the gearbox output, for example, exact harmonics of all signal components will not necessarily be contained within several revolutions of the output shaft. It is important that the width of the analysis intervals be chosen to reflect the signal's periodicity. Since transmission ratios often include prime numbers, the record length required for the periodic signal may be quite long. A side effect of longer analysis interval lengths is that relatively few non-overlapping spectra will result. In addition, a background speed ramp may be present in the time history data which can generate spurious harmonics in the FFT analysis. To overcome these problems shorter record lengths may be taken and a window function applied to remove sudden transients at the ends of the analysis intervals. Various window shapes may be used with the Hanning window being the most versatile [3]. Although FFT windowing reduces the leakage error it causes both damping of spectral-line amplitudes and broadening of the lines. The former may be corrected for by the RAS software based on the FFT window characteristics. The broadening of spectral lines cannot be corrected. In summary, periodicity in the analysis intervals for order analysis may be ensured by setting the interval length to a finite number of revolutions of the source of the vibration. However, frequency analysis on arbitrary time intervals requires the use of FFT windowing functions.
Two applications requiring multichannel measurement and analysis will now be presented in order to illustrate the capabilities of RAS equipment.

Timing Belt Drive System Optimisation

The primary purpose of synchronous belt drive systems is to synchronise camshafts and crankshafts. The belt system may also be used to drive integrated auxiliaries. In the 4-cylinder diesel engine shown in Figure 8 the crankshaft pulley drives the camshafts via a toothed belt. The idler on the tight side ensures that the belt wraps properly around the crankshaft's toothed wheel. The tensioner on the slack side provides tension. The fuel pump is also integrated into this drive system.

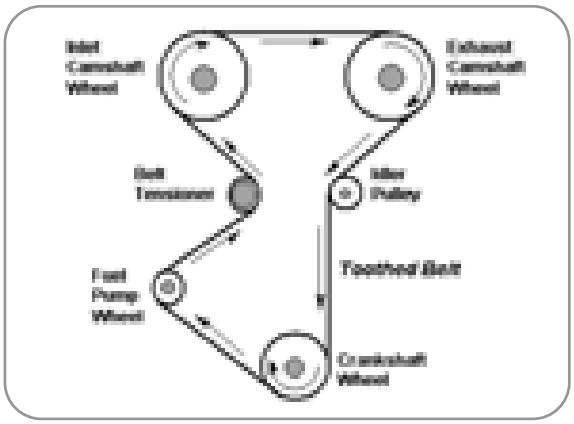

Figure 8 *Synchronous Belt Drive System*

The rotational speed of the crankshaft, fuel pump and camshafts was measured by scanning their toothed wheels with magnetic proximity sensors. The sensors operate up to a sensing gap of 5mm which allows for detection through the belt. In addition, displacement and force sensors provided analogue voltage signals from the tensioning system.
The interaction between the components is important when optimising the system's dynamics. With the aim of minimising the dynamic load on the drive system, loads and forces in the system as well as torsional and linear vibrations need to be investigated in detail. The most versatile tool for order domain analysis today is the speed/spectrum waterfall plot where a 3-D graphical display is used to visualise the orders as

they change frequency and amplitude with speed. An example of this is shown in Figure 9 in which torsional vibration amplitudes at the fuel pump wheel referenced to the crankshaft speed display a dominant second order.

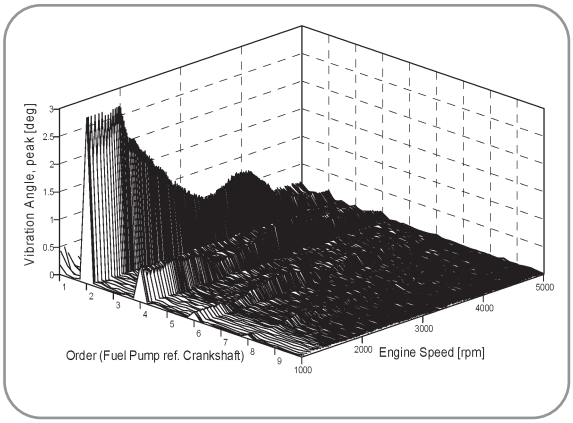

Figure 9 *Order Analysis – Waterfall Overview*

The influence of the effective tension (dynamic tight minus slack belt tension) on the life and durability of the belt is significant. Figure 10 shows the effective tension on the belt both before and after improvements were made to the system. Lower torsional vibration and belt tension fluctuation were present in the speed range around 3000rpm following improvements to the system.

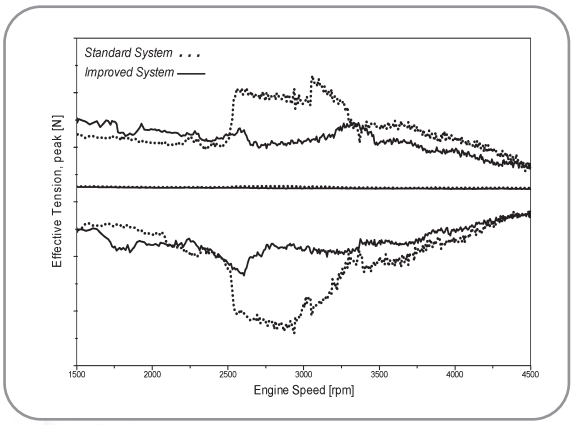

Figure 10 *Belt tension versus Speed*

Powertrain of a 4WD-Vehicle

One of the most comprehensive investigations made with RAS equipment to date involves the instrumentation of a four-wheel-drive vehicle test rig. The RAS system used was fitted with a total of 16 speed and 40 analogue channels as well as inputs for CAN-bus and triggering/pre-triggering signals. The flywheel teeth and synchronisation signals were used both to trigger data acquisition and provide a reference for the engine rotational position. The angular velocity of several gears within the gearbox was measured. Special toothed wheels were added to the shafts and scanned either with standard magnetoresistive sensors or with 4-fold sensors for improved resolution. The vibration of the gearbox casing was measured with ICP accelerometers. Additionally, force, temperature and displacement sensors were fitted. The instrumentation is outlined in Figure 11 where angular velocity measurement points are indicated by the symbol ω.

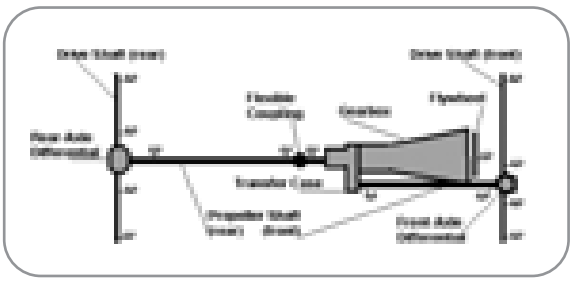

Figure 11 *Angular Velocity Measurement Positions*

Some objectives of the tests conducted were:

- Load change problems (vibration behaviour when switching from drive to coast)
- Transmission accuracy of differential gears
- Improving driving comfort by introducing vibration absorbers and a dual-mass flywheel
- Noise emission due to gearbox rattling

These types of multichannel investigations help in the understanding and interpretation of vehicle dynamics and provide ideal input data for validating computer simulations used in predicting and visualising engine and powertrain NVH behaviour.

Conclusions and Outlook

This paper reviewed and discussed several aspects of multichannel measurement and analysis of torsional vibration and related data. Shortening development cycles while simultaneously increasing the volume and diversity of noise and vibration testing constitute conflicting requirements in modern NVH engineering. This emphasises the pivotal role of state-of-the-art testing tools.

Both time constraints and physical limitations in accessing measurement positions mean that test engineers have little chance in practice of acquiring all-embracing experimental data. Information flow between testing and computational departments will therefore have to be improved and optimised. Only an integrated approach which combines mathematical modelling and experimental testing can help reduce the number of prototypes and further shorten development cycles [7].

References

[1] E.J. Nestorides, "A Handbook on Torsional Vibration", Cambridge University Press, 1958.

[2] H. Heisler, "Advanced Engine Technology", ISBN: 1 56091 734 2, Arnold Publishers, 1995.

[3] J. Derek Smith, "Gear Noise and Vibration", ISBN: 0-8247-6005-0, Marcel Dekker, 1999.

[4] S. Adamson, "Measurement and Analysis of Rotational Vibration and other Test Data from Rotating Machinery", SAE Paper No. 2000-01-1333

[5] S. Adamson, „Verbesserte Verfahren zur Messung und Analyse von Drehschwingungen", Expert Verlag 2003, ISBN 3-8169-2260-0

[6] RAS Manual, Version 5.0, ROTEC GmbH, 2003

[7] C. Weber, D. Beismann, S. Adamson and M. Prem, "Torsional Vibration Analysis of Internal Combustion Engines", MTZ Worldwide, March 2001

Improved Approaches to the Measurement and Analysis of Torsional Vibration.
Seán Adamson, Rotec GmbH.
From SAE World Congress, Detroit 2004. SAE Paper No. 2004-01-1723.

Torsional Vibration Analysis of Internal Combustion Engines

Carsten Weber, Dirk Beismann, Ford-Werke AG, Cologne · Seán Adamson, Markus Prem, Rotec GmbH, Munich

This paper describes the effects which both a torsional vibration damper and a dual-mass flywheel exert on crankshaft torsional vibration behaviour in a newly developed 4-cylinder 4-stroke in-line petrol engine. Typical system parameters which characterise the engine and critical operating points are discussed. Results of extensive experimental torsional vibration testing as well as data from a new simulation model are presented. Emphasis is placed on the comparison of measurement data and calculations in both the time and frequency domains in order to determine significant dynamic phenomena and their causes. The measurements were performed using a Rotec Universal Schwingungs Analysator (Vibration Analyser) (USA) in the John Andrews Development Centre of Ford-Werke AG in Cologne. The simulation model was developed by Rotec GmbH, Munich.

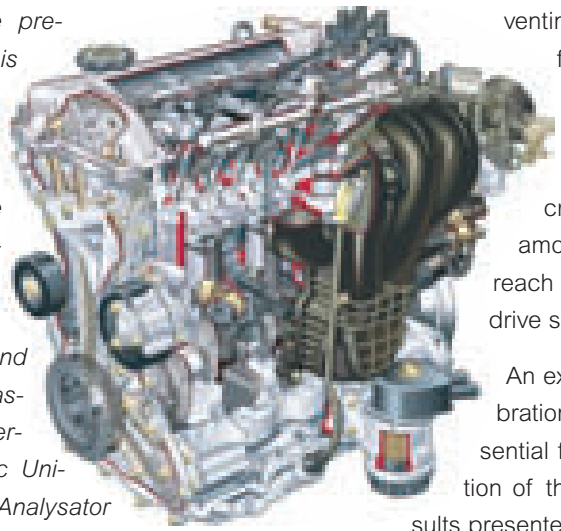

1. Introduction

Modern 4-stroke internal combustion engines are subjected to demands for increased efficiency, performance and reliability combined with an improvement in noise and vibration characteristics. This means that measuring and analysing the torsional vibration behaviour of the crankshaft is gaining in importance. The use of dual-mass flywheels for preventing vibrations generated by the engine from reaching the transmission and powertrain is increasing. Belt pulleys with integrated torsional dampers which are fitted to the front end of the crankshaft can also help in reducing the amount of crankshaft vibrations which reach valve trains, timing drive and auxiliary drive systems.

An exact understanding of the torsional vibration behaviour of the crankshaft is essential for the effective design and construction of the above-mentioned systems. The results presented below are based on detailed experimental work as well as numerical calculations.

2. Torsional Vibration Measurement

2.1 Test Engine

The experimental investigations of crankshaft torsional vibrations were performed on a Ford 2.0-litre Duratec HE engine. In 4-cylinder in-line engines of this type [8], torsional damper is integrated into the belt

pulley which is located at the front of the crankshaft. A newly developed dual-mass flywheel is also fitted to the crankshaft.

2.2 Measurement System and Measurement Set-up

Dynamic measurement of the rotational speed and hence torsional vibrations involves sampling at constant angular intervals around the rotating shaft and is accomplished here by using proximity sensors to scan the passing teeth of a toothed wheel. The signals obtained from this type of measurement contain information on the evolution in time of the instantaneous rotational speed. The USA system's measurement channels provide very high time resolution and possess a common time base to ensure accurate, synchronised measurements across many channels. The measurement channels operate in real-time with 32-bit resolution [1].

The common time base eliminates any time or phase errors and enables reliable order analyses of all quantities measured. Simultaneous measurement of the rotational speed at both ends of the crankshaft is necessary in order to be able to identify dynamic torsional vibration effects of the crankshaft drive which are caused by irregularities in belt pulley and dual-mass flywheel behaviour. Figure 1 shows the measurement set-up for investigating crankshaft torsional vibrations. At the flywheel end, the starter ring gear was used as a target for the speed measurement, whereas the trigger wheel was used at the crankshaft front end. Magneto-resistive sensors are used for non-contact measurement of the rotational speed.

Figure 2 shows a sensor positioned for scanning the passing teeth of the trigger wheel [3,4]. The frequency of the TTL signal generated by the conditioning

Figure 2 *Speed measurement at the trigger wheel using a magnetic sensitive sensor*

electronics is proportional to the angular velocity of the shaft.

The relatively low number of teeth on the trigger wheel allows order analysis up to engine order no. 10 to be performed without aliasing effects impairing the reliability of the results. Figure 3 shows the USA measurement and analysis system as well as the 2.0-litre Duratec HE engine. The investigations were performed on a test bed and data were continuously acquired for speed ramps in the range from 1000 to 6000 rpm with maximum engine load.

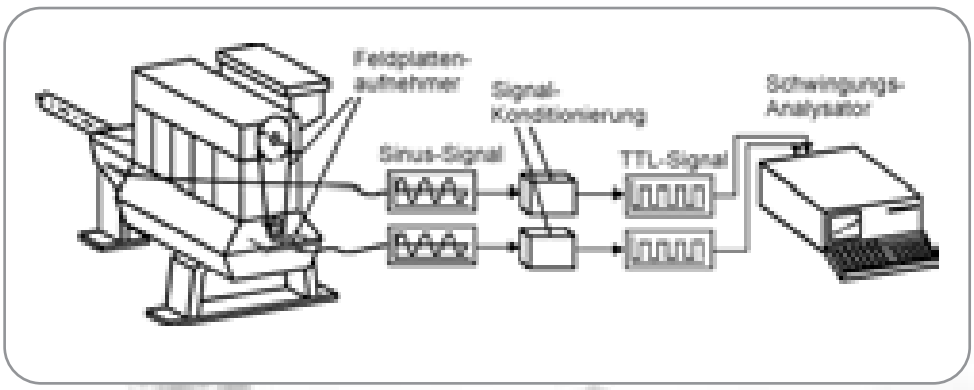

Figure 1 *Schematic assembly for torsional vibration measurement of the crankshaft*

2.3 Experimental Results

Figure 4 shows the results of a torsional vibration analysis obtained for three different crankshaft drive configurations of the Duratec HE engine.

The figure presents order spectra of the vibration angle measured at the crankshaft front end as a function of engine speed. The upper waterfall plot is for the case of a crankshaft drive with a conventional single-mass flywheel and rigid belt pul-

ley without an integrated damper. The spectra show a decrease in the second and fourth order vibration angle amplitudes with increasing engine speed. These orders result from engine firing. However, the amplitudes of both the fourth order and the remaining harmonics begin to increase again at an engine speed of about 3000 rpm. It is of note that the amplitude of the fourth order reaches a maximum towards the end of the speed ramp. The sixth, eighth and tenth orders have a maximum vibration amplitude at 4200, 3150 and 2520 rpm respectively. These maximum values result from superimposing the crankshaft drive harmonic excitation with the system's natural requency of 420 Hz. The latter is also visible running hyperbolically through the 3-D spectrum [5,6,7]. The second waterfall spectrum shows the positive effect which a damper tuned to the system's critical natural frequency can have on torsional vibration behaviour. The spectrum shows a significant reduction in the vibration amplitudes of the engine harmonics [2].

The purpose of the dual-mass flywheel is to prevent torsional vibrations generated by the engine from reaching the transmission and powertrain. At lower engine speeds, however, significantly higher rotational irregularity is measured at the crankshaft front end for the second and fourth engine orders. This is due to the low value of the engine-side primary mass. At the same time, the amplitudes of the fourth and sixth engine orders are reduced at higher speeds, as can be seen in the lower waterfall spectrum of Figure 4.

Figure 3 *Testbed setup for torsional vibration measurement at the crankshaft*

Figure 5 shows the effect of the reduction of engine-side inertia due to the dual-mass flywheel. The figure shows the time domain vibration angle data at the front end for a complete 4-stroke working cycle as a function of engine speed. Of particular note is the high amplitude of the second engine order at lower speeds. The single-mass flywheel limits the vibration angle to a value of 1.75° at the crankshaft front end, whereas fitting a dual-mass flywheel results in an increase to 2.75°. In Figure 6, the resonance behaviour of the crankshaft torsional vibrations is seen in detail in a 2-D plot of individual orders as a function of engine

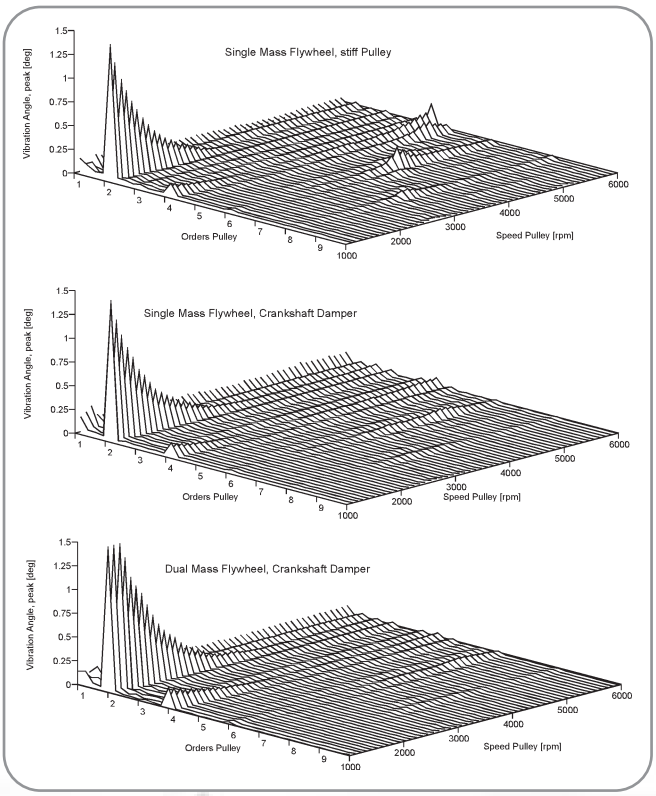

Figure 4 *Order Analysis of the measured torsional vibration*

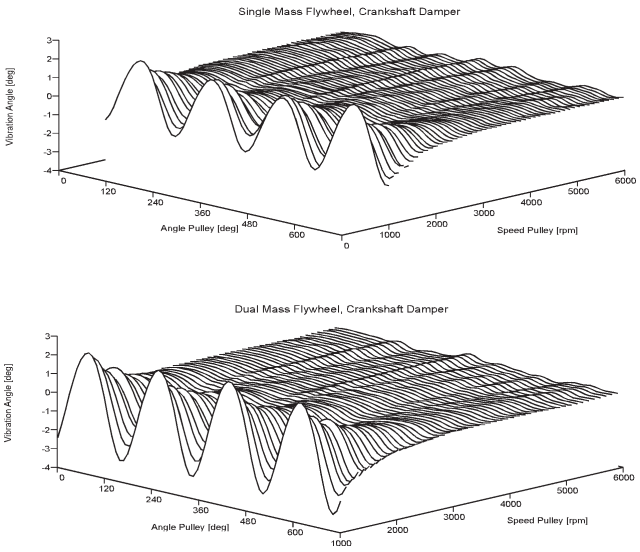

Figure 5 *Influence of the dual mass flywheel on the speed non uniformity*

speed. The curves in the upper diagram show the large amplitudes obtained for the shaft fitted with a conventional flywheel and rigid pulley. In particular, the sixth order dominates at 4200 rpm. Similar resonance effects are seen for the
fourth, eighth and tenth orders caused by the engine firing harmonics and system's natural frequency of 420 Hz. The second series of 2-D curves show how vibration amplitudes are clearly reduced when the crankshaft torsional damper tuned to the system's natural frequency is fitted. The previously dominant sixth order vibration amplitude is reduced from 0.22° to 0.05°. A further reduction in the torsional vibration amplitudes was achieved by fitting a dual-mass flywheel, Figure 6, lower series of curves. This is due to lower inertia on the engine side causing an upward shift of the system's natural frequency from 420 Hz to 458 Hz.

3. Simulation

3.1 Model

Using the simulation software, models can be created which are based on fundamental elements such as masses, spring dampers, transmission ratios and earth sinks. These elements may be linked to create straight, branched and meshed structures. Initialising an excitation is accomplished using either a frequency sweep, a list with excitation forces or real data from a measurement channel. The calculations are linear and run as a function of frequency. Relatively short simulation times are thus realised by transforming discrete sections into the frequency domain. The results of a calculation are either 2-D or 3-D curves, for example, the vibration angle versus both engine speed and order for an element. Figure 7 shows the torsional vibration model of the crankshaft drive including a dual-mass flywheel as investigated in the present work. Excitation of the model is accomplished by using the measured gas pressures as a function of angle and speed for each cylinder. Additionally, the inertias, stiffnesses, damping coefficients and crankshaft drive kinetics are also considered in the calculations [1].

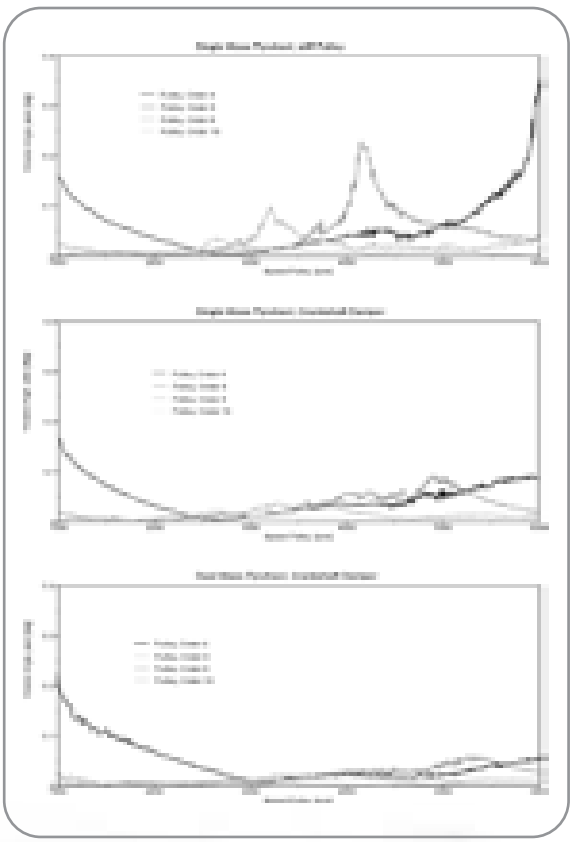

Figure 6 *Dominant single orders versus speed*

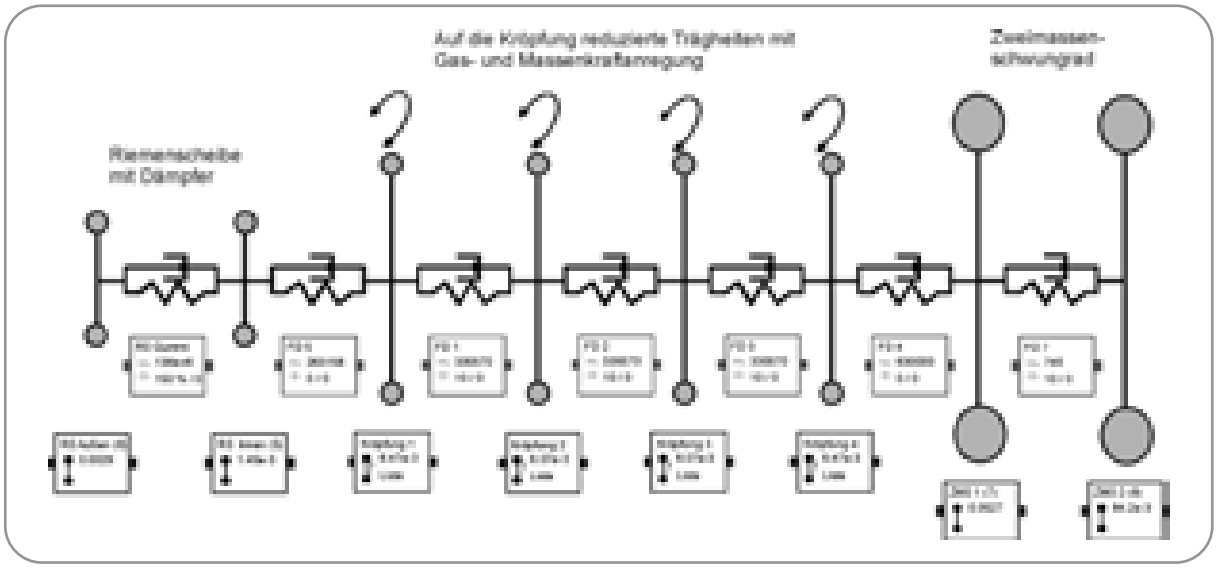

Figure 7 *Modell of the crankshaft to simulate torsional vibration properties*

3.2 Simulation Results

Analogous to the analysis of the measurement data, the order spectra shown in Figure 8 show the results of the simulation calculations for the crankshaft drive configurations considered. Comparison with Figure 4 shows that excellent agreement between measurement and simulation is obtained for torsional vibration levels at the front end of the crankshaft.

The order spectrum for the case of a single-mass flywheel and rigid pulley, upper spectrum of Figure 8, is dominated by the system's natural frequency. Using the simulation program to calculate the system's natural frequency yields a value of 425 Hz, which correlates very well with the values obtained experimentally.

Including a tuned crankshaft damper in the simulation model also produces a significant reduction of the sixth order vibration angle at 4250 rpm. The lower spectrum of Figure 8 shows the results of the calculation with the dual-mass flywheel also included. Reduction of the vibration angle amplitudes for orders 4, 6 and 8 is also seen, as is an increase in rotational fluctuation at low engine speeds.

4. Summary

Torsional vibration amplitudes in the region of the system's natural frequency were reduced by 75% by integrating a torsional damper into the belt pulley at

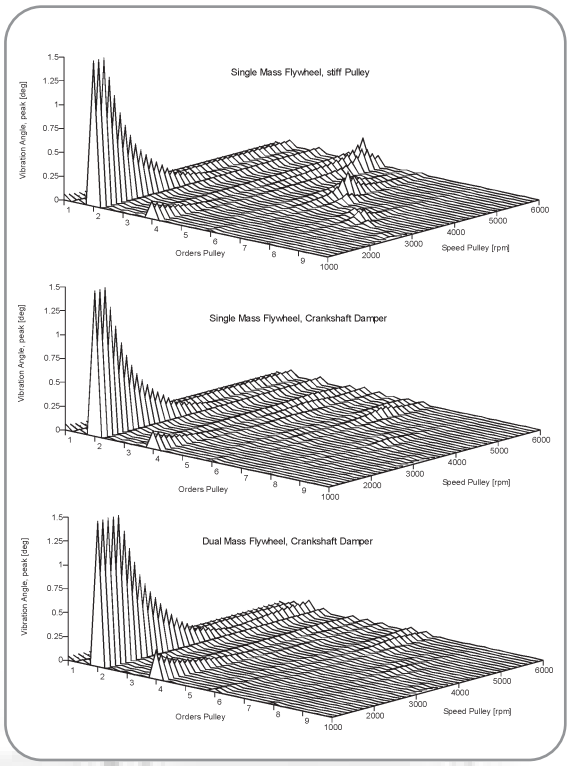

Figure 8 *Order analysis computed by the simulation software*

the crankshaft front end. When a dual-mass flywheel was fitted, a minimal increase in the vibration level was observed at the shaft's front end at low speeds. Simultaneously, because of the lower engine-side inertia, the natural frequency was shifted upwards by 38 Hz. This also contributed to a further reduction of torsional vibration amplitudes in the range of medium and high speeds.

The simulation calculations reliably predict the torsional vibration behaviour of the crankshaft configurations which were experimentally investigated. Very good agreement was obtained between the experimental results and the results of the simulation calculations carried out in the frequency domain. Numerical parameter studies therefore offer a time-saving possibility for calculating the torsional vibration characteristics of engines. By combining both simulation and experimental testing, the number of prototypes required in the development of new engines may be reduced and the requirement of shorter development cycles will thus be achieved.

Literature

[1] N.N. Bedienungsanleitung RAS/USA Schwingungsanalysator der Firma Rotec GmbH, München, 2000

[2] Glaser, H.: Ein neues Torsionsschwingungsverfahren zur Dimensionierung eines verschleißarmen Drehschwingungstilgers im Antriebsstrang eines Allradfahrzeuges. VDI-Berichte 791, VDI-Verlag, Düsseldorf 1990, 57-76

[3] Adamson, S.: Schwingungen an Antrieben messen. In: Werkstatt und Betrieb 129 (1996), Carl-Hanser Verlag, München

[4] Adamson, S.: Measurement and Analysis of Rotational Vibration and other Test Data from Rotating Machinery. In: SAE 2000 World Congress, Detroit, März 2000.

[5] Weber, C.; Herrmann, W.; Stadtmann, J.: Experimental Investigation into the Dynamic Engine Timing Chain Behaviour. SAE 1998 World Congress, Detroit Februar 1998

[6] Weber, C.; Beismann, D.; Hentrich, D.; Herrmann, W.; Stadtmann, J.: Investigation into the Dynamic Engine Timing Chain Behaviour. Global Powertrain Congress, Stuttgart, Oktober 1999

[7] Weber, C.: Drehschwingungsmessung und deren Analyse an Verbrennungsmotoren. Seminar für Festkörpermechanik TU Dresden, Juli 2000

[8] Tielkes, U.; Menne, R. J.; Hügen, S.; Hansen, J.: Die neue Ottomotorengeneration Duratec HE von Ford. In: MTZ 61 (2000), Nr. 10, S 646-654

Torsional Vibration Analysis of Internal Combustion Engines. Carsten Weber and Dirk Beismann, Ford-Werke AG, Cologne. Seán Adamson and Markus Prem, Rotec GmbH, Munich.
From MTZ Worldwide (Motortechnische Zeitschrift 62/2001) 3

Upgrading a Gear Testing Machine for use in Single Flank Testing and Airborne & Structure-Borne Noise Measurements

Rotec GmbH, Munich

1. Introduction

The machine in question was primarily designed for contact pattern imaging of gearsets (Figs 1 and 2). The contact patterns are evaluated by eye. The rotational speed of the drive side is set to a given speed and the output side is braked manually in order to load the gearset and ensure constant tooth surface contact.

This procedure relies to a large extent on the skill of the operator. To replace this largely subjective and qualitative approach with quantitative testing methods it was decided to modify and upgrade the machine in order to make both single flank testing and the measurement of airborne and structure-borne noise possible. This involved both the introduction of new instrumentation and the mechanical modification of the machine which may be summarised as follows:

- Fitting of a magnetic particle brake onto the end of the output shaft to provide constant and reproducible braking moments.
- Incorporation of a high-resolution incremental encoder into both the input and output spindles to provide signals for transmission error measurements.
- Positioning a microphone in the vicinity of the gearset for provision of airborne noise signals.
- Adding an accelerometer to the driven side spindle housing for provision of structural noise signals.
- Employing a rotec-RAS measurement and analysis system for high-resolution, synchronous acquisition of the incremental encoder, microphone and accelerometer signals.

Figure 1 *The machine before any modifications were carried out. The photo shows the input and output spindles and the location of the hand-brake on the output side.*

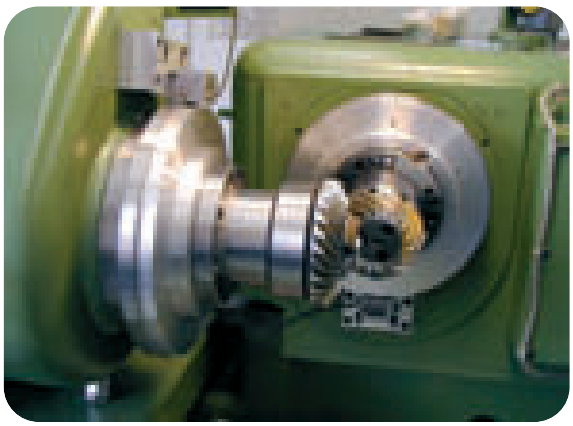

Figure 2 *Close-up of a gearset showing contact image patterns on the tooth surfaces.*

2. Gear Noise and Transmission Error

Gear noise is a major concern in the design and manufacture of gearsets. A pair of gears should transfer angular motion uniformly and the Transmission Error is defined as the difference between the actual position of the driven gear and the position it would occupy if the gearset were perfectly conjugate. It is generally accepted that Transmission Error is the main cause of gear noise.

2.1 - Single Flank Testing

The Single Flank Test is a two-channel rotational speed measurement. The measurement is performed by integrating high-resolution rotary encoders into the shafts of the driving and driven gear wheels (pinion and gear). By definition, single flank testing is performed at low rotational speeds (approx. 20 rpm). A load is applied by braking the driven side which ensures constant tooth surface contact. The angular positions of both pinion and gear are then recorded by measuring the time intervals between encoder lines. The transmission error curve results from the deviation in rotating angle between the signals from the two encoders taking the transmission ratio into account. The patterns in the transmission error curve originate from eccentricity (runout) in rotation of the pinion and gear and from the tooth meshing. This is observed in the form of a fairly regular once-per-tooth pattern superimposed on larger waves which are related to once-per-revolution type errors. The once-per-tooth (or faster) short wave components of the curve result from tooth meshing problems caused by surface structure effects and tooth geometry. The long wave portion is due to runout errors. Additionally, components due e.g. to support structure bolts may be present which bear no relationship to tooth geometry.

2.2 - Airborne Sound and Structural Noise Analysis

In order to obtain a more complete picture of the gearset's running behaviour additional signals may be acquired synchronous to the encoder data. Such signals often include structural noise on the bearings and airborne sound.

3. Upgrade

3.1 - Instrumentation

Rotation Analysis System rotec-RAS

Rotec GmbH, located in Munich Germany, specialises in the design and manufacture of portable, pc-based equipment for the measurement and analysis of noise and vibration. The Rotation Analysis System RAS (Figure 3) is designed for synchronised multi-channel acquisition and analysis of both digital and analogue signals. Digital signals originate from rotational speed sensors whereby analogue signals are provided by accelerometers, microphones, strain gauges etc. A 100MHz quartz oscillator serves as time base for all RAS measurement channels to ensure that accurate, synchronised measurements across all channels are achieved. This eliminates any time or phase errors when performing cross-channel analysis.

When performing single flank testing with the RAS each single graduation line on the encoders is evaluated and an exact reproduction of tooth meshing patterns results. Since order analysis of all data is possible, accurate correlation between, for example, noise levels and tooth meshing may be made. [1,2].

When performing single flank testing with the RAS each single graduation line on the encoders is evaluated and an exact reproduction of tooth meshing patterns results. Since order analysis of all data is possible, accurate correlation between, for example, noise levels and tooth meshing may be made. [1,2].

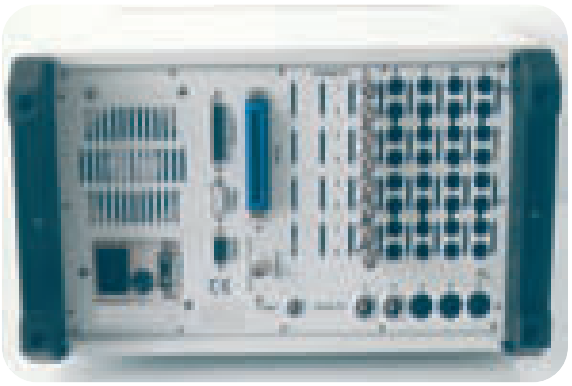

Figure 3.2 *RAS Rear Panel*

Figure 3.1 *RAS Front Panel*

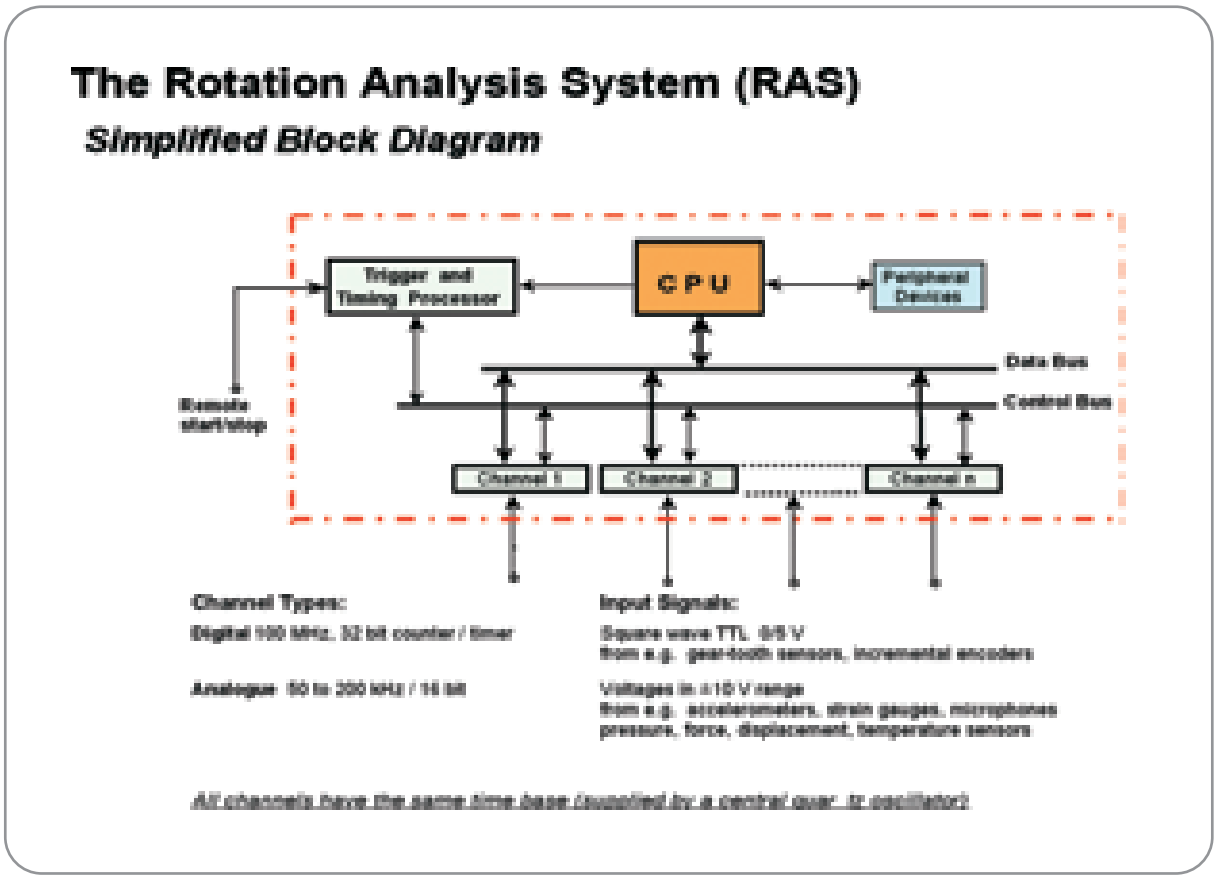

Figure 3.3 *RAS Schematic*

Incremental Encoders, Accelerometer and Microphone

Figure 4 shows pinion and gear wheels mounted on input and output spindles. The microphone is located slightly above the two wheels. An incremental rotary encoder is integrated into both the input and output spindles (screened from view). An accelerometer is mounted on the output spindle bearing (also not visible). The specifications are as follows:

- Incremental rotary encoders: line count 2048.
- Microphone: sensitivity 25 mV / Pa.
- Accelerometer: sensitivity 1000 mV / g, range 5g.

Figure 4 *Microphone positioned above gearset mounted on input and output spindles.*

3. 2 - Magnetic Particle Brake

The magnetic particle brake fitted to the end of the output shaft is shown in Figure 5. The brake is capable of generating braking moments up to 30Nm and ensures constant moments independent of rotational speed. The brake assembly unit is resistant to wear and requires minimal maintenance. The moments are directly proportional to the electric current supplied. This current is set with a rotary switch on the brake's control unit. Current values are recorded by the RAS system, converted to moments and protocolled for further analyses. An overview of the upgraded machine including the RAS system is shown in Figure 6.

Figure 5 *Magnetic particle brake assembly.*

Figure 6 *Overview of the upgraded machine.*

4. Results

The rotec-RAS system was used for acquisition of the TTL pulse train signals from the rotary encoders and voltage signals provided by the accelerometer, microphone and brake control unit. Comprehensive RAS data acquisition and analysis software allows the user to easily configure the test and document the results. Gearset parameters, rotational speed, braking moments, amplitudes of tooth mesh orders,

harmonics of tooth mesh, ghost harmonics, DIN characteristic values, etc. may be easily protocolled to produce, for example, a single line of information per gearset and a complete protocol file per shift.

The RAS system is fitted with an Ethernet interface which allows viewing of the test protocols from external PCs. This enables continuous monitoring of the quality of gearsets during production runs.

Single Flank Testing

The following notation is based on German DIN Standards (original German terms in italics).

F'*i* total or cumulative transmission error (Einflanken-Wälzabweichung)

f'*l* long wave component (langwelliger Anteil)

f'*k* short wave component (kurzwelliger Anteil)

f'_{max} maximum value of tooth-to-tooth error (Einflanken-Wälzsprung)

In addition, f' mit = average value of tooth-to-tooth error is calculated.

References

[1] RAS, Version 3.6 User's Manual, Rotec GmbH, Munich, 2000

[2] S. Adamson, "Measurement and Analysis of Rotational Vibration and other Test Data from Rotating Machinery", SAE Technical Paper No. 2000-01-1332

Upgrading a Gear Testing Machine for use in Single Flask Testing and Airborne and Structure-Borne Noise Measurements.
Rotec GmbH Application Note, July 2000.

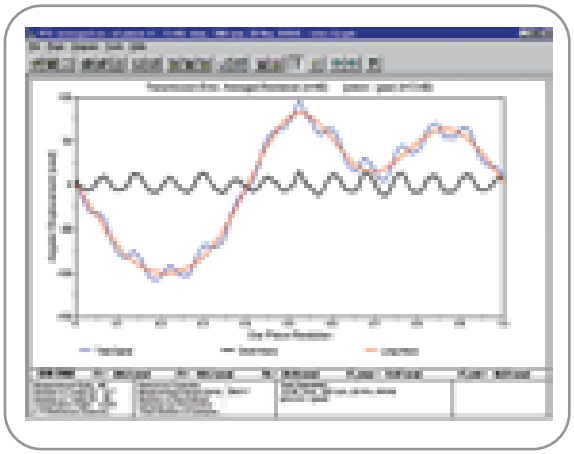

Figure 7 *The transmission error curves show the deviation between the actual position of the driven wheel and the position it would occupy if the gearset were perfectly conjugate.*

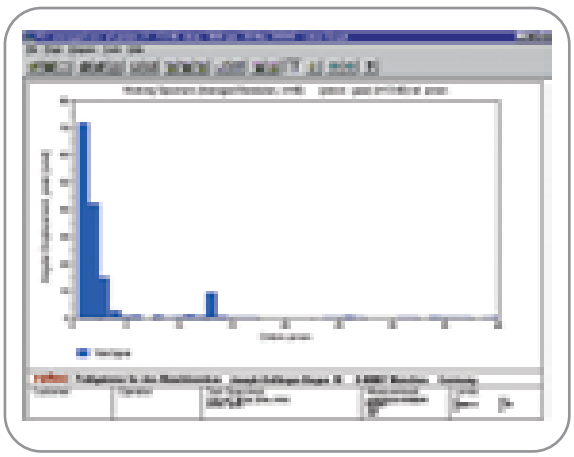

Figure 8 *The spectrum of the total transmission error includes the tooth meshing order, its harmonics and side bands.*

Measurement and Analysis of Rotational Vibration and other Test Data from Rotating Machinery

Seán Adamson, Rotec GmbH, Munich

Abstract

When collecting torsional vibration and other test data, many automotive testing departments utilise a combination of hardware and software tools whereby each tool is dedicated to a specific physical phenomenon. Following a series of measurements, the various data are merged for correlation and computer-aided analysis: a procedure which can be cumbersome and time-consuming. In addition, it can lead to errors when performing cross-channel time or phase analyses since all data will not necessarily have been collected on the same time base. In this paper, a portable pc-based data acquisition and analysis system is described which allows for reliable synchronised multi-channel acquisition and analysis of both torsional vibration and a variety of related signals.

Introduction

In the automotive industry, when developing and testing engine and power transmission systems special attention is given to the measurement and analysis of both rotational and transverse vibration quantities. Achieving a better understanding of the causes of noise and vibration problems contributes to reducing component wear, increasing ergonomic comfort and optimising vehicle design and performance. Over the past decade, Rotec GmbH, located in Munich, Germany, has specialised in the design and manufacture of pc-based equipment which specifically addresses the needs of test and development engineers in automotive engineering. The system presented here, the Rotation Analysis System (RAS), enables synchronised multi-channel acquisition and analysis of both digital and analogue signals [1]. The digital signals (square wave TTL) are provided by rotational speed sensors whereas analogue signals (±10V range) originate from, for example, accel-erometers, pressure, force and acoustic sensors. By measuring and analysing several types of physical phenomena with the same instrument, more accurate and reliable understanding of their origins is achieved. In addition, development and testing cycles are made shorter and more efficient. The RAS analyser is used extensively in engine and powertrain development for both in-vehicle and NVH laboratory testing. This paper will discuss three applications (i) investigation of torsional vibrations of the crankshaft, (ii) single flank testing of gears and (iii) optimising belt drive systems.

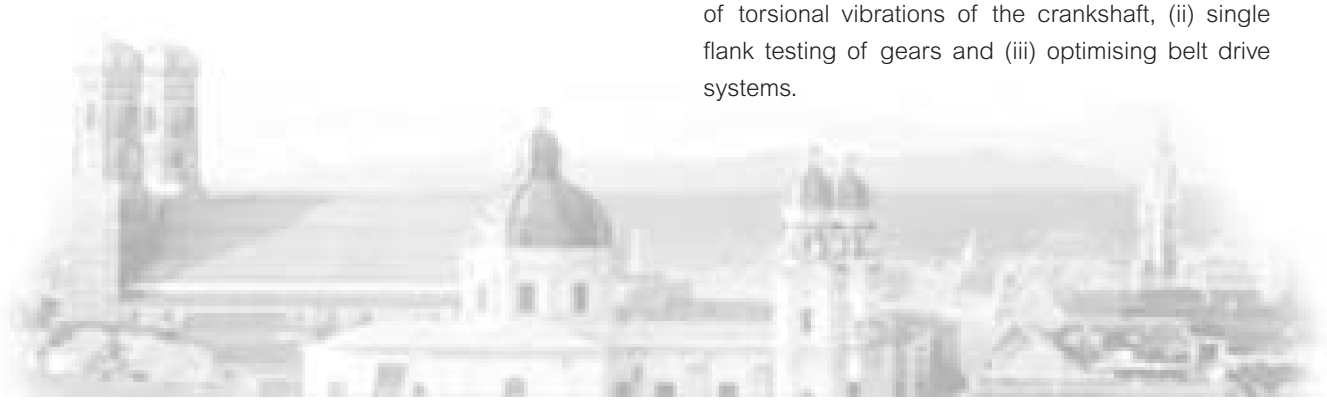

The RAS-Analyser

The Rotation Analysis System (see photo of Figure 1) is contained in a 3/4 19" robust metal case with fold-out keyboard. A colour LC display and floppy and magneto-optical disk drives are integrated into the front panel. The system currently contains a 9Gb hard drive and is based on a Pentium CPU with 128Mb of memory. Connectors for signal inputs are located on the rear panel which also contains a trigger input for remote start/stop of measurements.
Also integrated are serial, parallel, SCSI and ethernet ports. The supply voltage ranges from 110 to 230 VAC or, alternatively 9 to 32 VDC. A battery back-up ensures uninterruption of power supply. The RAS is fitted with data acquisition boards with integrated digital signal processors. A 100 Mhz quartz oscillator serves as time base for all boards to ensure that accurate, synchronised measurements across all channels are achieved. This eliminates any time or phase errors when performing cross-channel analysis [2].
The digital boards are single-channel and operate with a 100MHz, 32-bit counter/timer allowing for direct input of dynamic rotational speed signals in the form of rectangular TTL level pulse trains. The pulses represent constant angular intervals around the rotating shaft and provide information on the evolution in time of the instantaneous rotational speed. Magnetic pick-ups which detect the passing teeth of a toothed wheel, or optical rotary encoders integrated onto the shaft may be used as speed sensors.

Two types of analogue board may be fitted: An 8-channel board which samples at 50kHz per channel and a twochannel board with 200kHz per channel. The input voltage range is ±10V with 16 bit resolution per channel. Digital downsampling, anti-aliasing filtering, programmable gain, AC/DC coupling and selectable differential, isolated or ICP inputs are provided for. A simplified block diagram of the RAS system is shown in Figure 2.

Figure 1 *The Rotation Analysis System (RAS)*

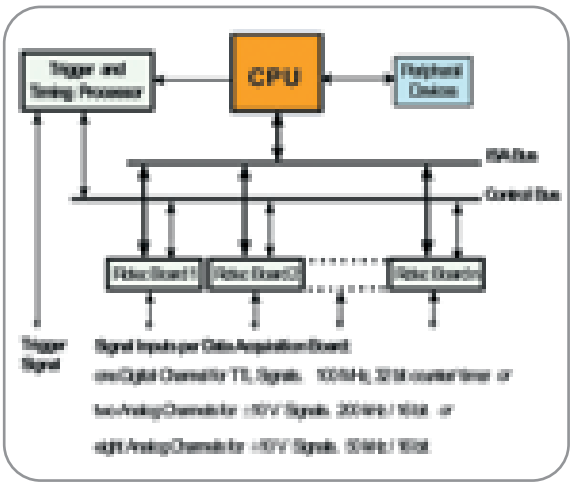

Figure 2 *RAS - Simplified Block Diagram*

Software

The RAS software is 32 bit Windows based and provides the user with a powerful tool for data acquisition and analysis. Real-time analysis with display of spectra is possible during measurements. All data are initially stored in on-board memory as time histories before transfer to hard disk following the measurement. This raw time data is then available for analysis on the RAS itself or on an office PC.
Comprehensive software for both time and spectral domain analysis is provided. All quantities may be represented as a function of time, angle or rotational

speed. For torsional vibration channels the speed variation, angular velocity, vibration angle and angular acceleration may, for example, be calculated. Multi-channel speed measurements enable angular displacement, transmission error, slip and speed differences between selected channels to be calculated. Analogue signals may be frequency analysed versus time and order analysed referenced to a selected speed channel. Dedicated software modules include: single flank testing of gearsets, compensating for missing teeth, acoustic and statistical analyses.
The RAS software also provides for creation of models of test specimens which may then be animated with real measurement data. The test engineer may thus quickly gain an overview of phase relationships in complex systems such as belt drives. A simulation program is also available with which predictions of mathematical models may be compared with actual test results [3]. The RAS system, therefore, constitutes a dedicated tool for measurement, analysis, animation and simulation which significantly aids the test engineer in quick identification of the nature of transmission system problems.

Order Analysis of Torsional Vibrations

Measuring and analysing torsional vibrations of the crankshaft is important in the understanding of dynamic problems encountered in the design of combustion engines. The vibrations are caused by fluctuations in torque which are created by the so-called mass and gas forces. The mass forces result from piston, connecting rod and crankshaft movement; the gas forces from pressure within the cylinders. Single-channel measurement of the engine's rotational speed is often performed at the front end of the crankshaft. The case presented here involves a 4-cylinder, 4- stroke diesel engine. It was not possible to use a rotary encoder due to difficult environmental factors (rugged operation, dirt) so that the combination of toothed wheel and differential magnetoresistive speed sensor had to be used. A ferromagnetic toothed wheel with 200 teeth and of 7mm thickness was bolted to the crankshaft and was scanned by the speed sensor at a distance of about 2mm. The sensor's conditioning electronic unit operates up to 50 kHz tooth frequency and generates a rectangular wave TTL signal for input to the RAS analyser (Figure 3). Frequency (order) resolution depends on the target wheel's number of teeth whereas amplitude resolution is determined by the clock frequency of the counter/timer board. It is instructive to consider the effect that rotational speed, number of teeth and clock frequency have on angular resolution. The RAS directly measures the time interval between positive edges of incoming TTL pulse trains. Take, for example, a wheel with 200 teeth rotating at 3600 rpm. The tooth frequency is

$$(3600 / 60) \times 200 = 12 \text{ kHz}$$

If the wheel is scanned by a proximity sensor which produces TTL pulses then the number of 10ns clock counts between adjacent positive edges is

$$(100 \times 10^{6}) / (12 \times 10^{3}) = 8333 \text{ counts}$$

This results in a speed resolution of

$$3600 \text{ rpm} / 8333 = 0.43 \text{ rpm}$$

The angular resolution in this case would be

$$(1.8^{\circ} / 8333) = 2.2 \times 10^{-4} \text{ degrees}$$

↑ ↑
toothed wheel RAS time base

It should be noted that toothed wheels are often quite poorly machined. To alleviate this problem, Rotec has developed a special software routine which can determine and compensate inaccurate tooth spacing on the target wheel. It should be emphasised, however, that for more accurate work such as single flank testing of gearsets, rotary encoders are preferable as sensor.

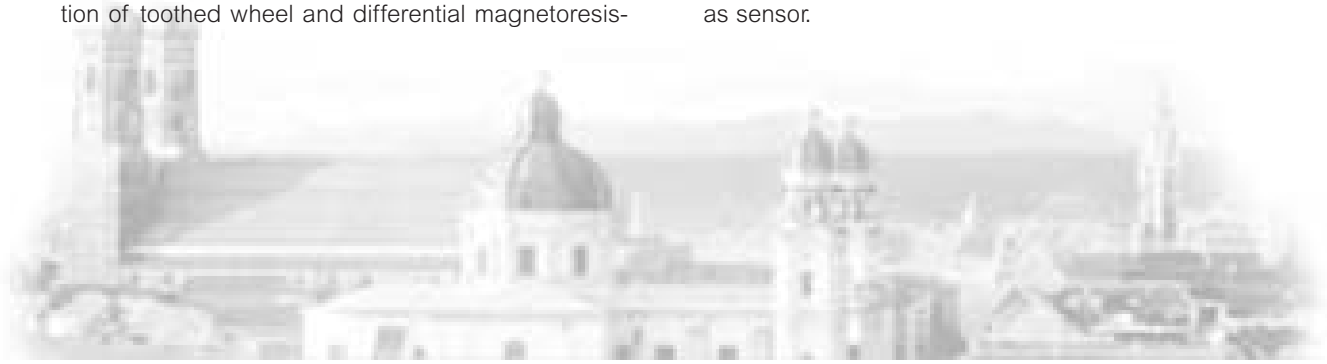

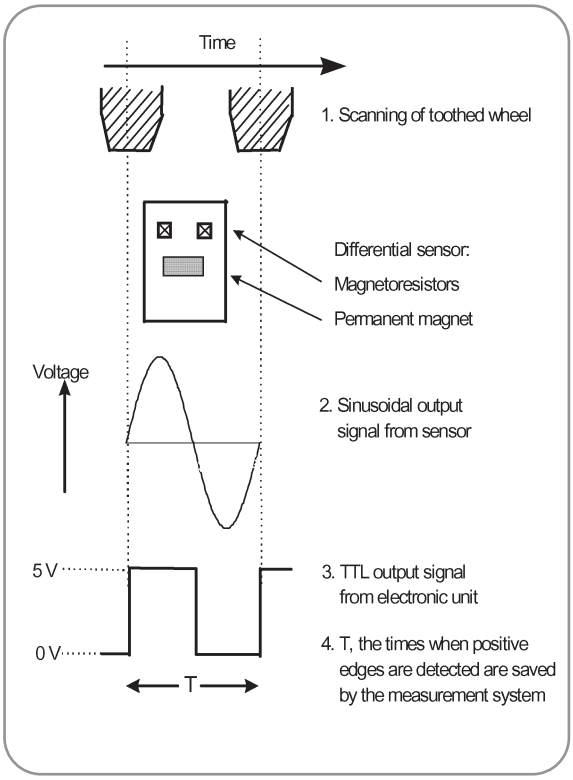

Figure 3 *Schematic diagram describing the operation of a differential gear tooth sensor.*

When analysing rotational speed data, the RAS software performs FFT analysis on data blocks which contain an integer number of revolutions. For order analysis of combustion engine signals, blocks of four revolutions are usually taken which results in 1/4 order resolution. This procedure means that the signals within the blocks are purely periodic. Leakage errors do not arise so that artificial windowing is not needed. However, the RAS software also provides for windowing (Hanning, Flat Top, etc.) of time samples of equal length when, for example, frequency analysis of analogue signals is to be performed. Analogous to order resolution, the frequency resolution in Hz is given by the recipricol of the block length in seconds.

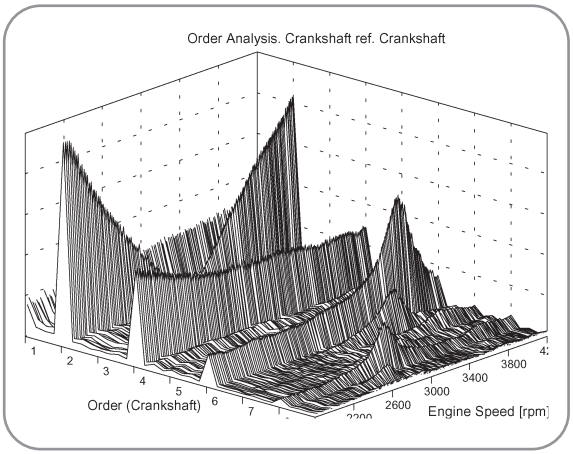

Figure 4 (a) *Diesel Engine Run-up. Waterfall plot*

The 3D waterfall plot (Figure 4a) gives a comprehensive display of evaluated data. Overviews of this type are especially suitable when investigating new test objects since information on critical operational states can be quickly obtained. For 4 (and 8) cylinder engines, half engine order multiples (1.5, 2.5 etc.) are due to the socalled gas forces while the mass force contributes predominantly to the harmonics with whole numbers.

The Campbell plot (Figure 4b) also displays the entire evaluated data, but in this case a 2D plotting style is employed. The amplitudes which appear as 'ridges' in the 3D variation, are in this case displayed as rectangles; the larger the area the higher the amplitude at the corresponding frequency/speed data points. The Campbell plot enables easier differentiation between orders and constant frequency structural resonances. This is of particular importance since excessive levels of resonance can cause component failure. Both overviews give the test engineer important indications on the presence of unwanted and possibly destructive vibration. For more detailed scrutiny, individual order lines can also be viewed (Fig. 4c)

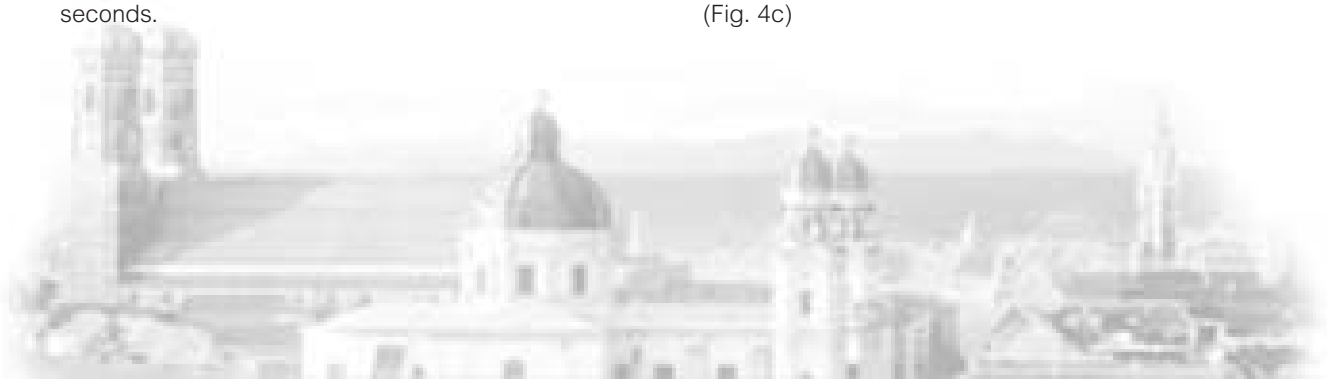

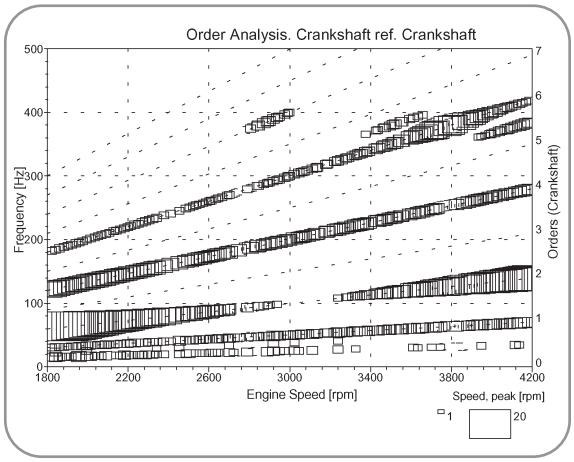

Figure 4 (b) *Diesel Engine Run-up. Waterfall plot*

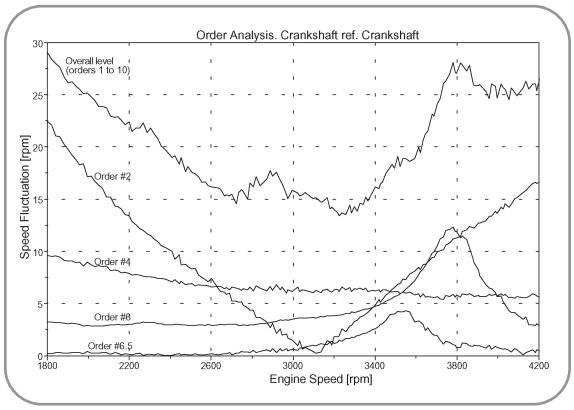

Figure 4 (c) *Diesel Engine Run-up. 2D order analysis*

Single Flank Testing of Gears

A pair of gears should transmit rotary motion uniformly from the drive shaft to the driven shaft. Single flank testing investigates the rotational movement of the axes of a pair of gear wheels and numerically describes the irregularities in transmission. The measurement is generally performed by integrating high-resolution optical rotary encoders into the shafts of the driving and driven gear wheels (pinion and gear). A two-channel speed measurement is then performed with the RAS.

The transmission error curve results from the deviation in rotating angle between the signals from the two encoder channels. The patterns in the transmission error curve originate from eccentricity in rotation of the pinion and the gear shafts and from the tooth meshing. This is observed in the form of a fairly regular once-per-tooth pattern superimposed on large waves which are related to once-per-revolution type errors (Fig. 5). The once-pertooth (or faster) short wave components of the curve, result from tooth meshing problems caused by surface structure effects and tooth geometry. The long wave portion is due to run-out errors. Additionally, components due e.g. to support structure bolts may be present which bear no relationship to the tooth geomerty.

Ideally, data should be recorded for at least one complete over-rolling of the two wheels. Angular averaging can be performed whereby consecutive pinion revolutions are averaged together. The long wave portion of the resulting total error curve is then isolated by using a low pass digital filter with a cut-off order selected to reject tooth mesh and higher frequencies (set normally at 1/3 tooth mesh). The short wave portion is obtained by subtracting the long wave components from the total error. Figure 6 shows the spectrum of the total signal of the averaged pin-

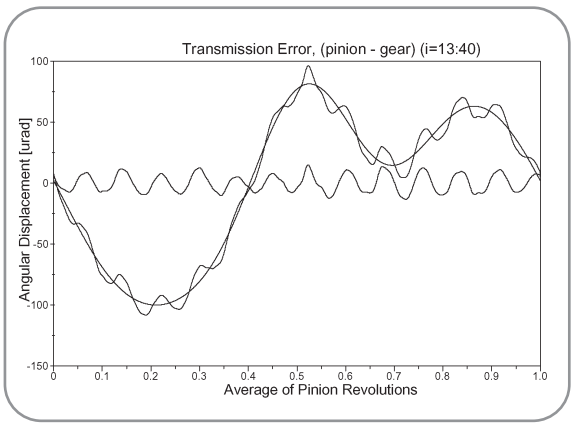

Figure 5 *Transmission Error Curves*

ion revolution. The pinion is used for order referencing. Tooth mesh is clearly seen at order 13 without significant side bands. In order to attain a more complete picture of the gearset's running behaviour, analogue signals may be recorded synchronous to the encoder data. Analogue data can include angular acceleration of pinion and gear, structural noise on the bearings and airborne sound. Since order analysis of all data is possible, accurate correlations between, for example, sound level and the gearset's running behaviour may be made.

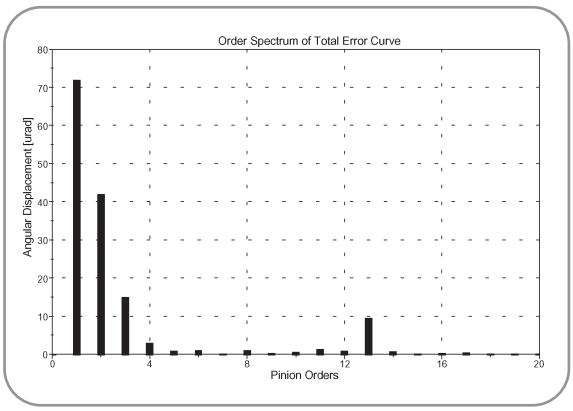

Figure 6 *Order Spectrum of Total Transmission Error*

Belt Drive System Optimisation

The multichannel capability of the RAS may be exploited when performing measurements on engine belt drive systems. Typically, rotational speed data are acquired at a number of points (crankshaft pulley, camshafts, fuel pump, alternator, etc.). In addition, linear data such as tensioner movement may be synchronously acquired. Analyses of interest are, for example, belt slip between pulleys or tensioner movement as a function of speed. Depending on the drive system's complexity and the test engineer's familiarity with it, comprehensive evaluation towards reaching a full understanding of all system components and their behaviour can be quite time consuming. RAS animation software provides the user with a tool for creating 3-dim models of the system undergoing test. The models may then be animated with real test data. The animated data can be observed for a complete engine run-up to provide an overview of amplitude and phase relationships as a function of engine speed. Figure 7 shows an example of a 6-cylinder engine where the auxiliaries are driven by a ribbed V-belt. Torsional vibration was measured by scanning toothed wheels at four positions: crankshaft, power steering pump, air-conditioning compressor and anternator. Data from a travel sensor attached to the belt tensioner was also taken. Following the measurement the third order referenced to crankshaft speed was calculated for all channels (vibration angle for speed channels, belt tensioner movement for the analogue channel). This data was then linked to the model to give an overview of vibration amplitude and phase behaviour over the course of the measurement. Of particular note in the case presented here was excessive belt movement caused by the crankshaft and alternator pulleys being out-of-phase at certain critical speeds.

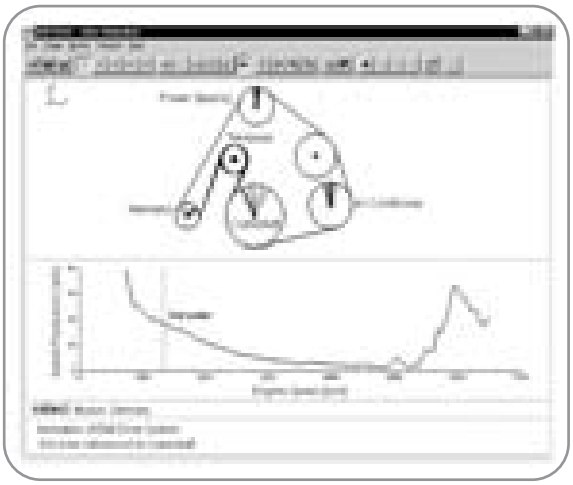

Figure 7 *Animation Model of Belt Drive System*

Conclusion

The Rotation Analysis System has been shown to be a valuable measurement and analysis tool for assessing the characteristics of noise and vibration and relating critical conditions to the speeds at which they occur. Synchronous acquisition of all data with the same instrument improves the accuracy and reliability of results. Animation of test data is a novel method of attaining an overview of amplitude and phase relationships in complex systems.

The integration of accurate test data collected under operational conditions into both animation and simulation models will help even more in the prediction and understanding of rotating machinery behaviour.

References

[1] "RAS Version 3.5 User's Manual", Rotec GmbH, Munich, 1999

[2] S. Adamson, S. "Schwingungen an Antrieben messen". Werkstatt und Betrieb 129, Nov. 1996. Published by Carl-Hanser Verlag, Munich

[3] S. Adamson, to be published

[4] J. Williams, "Improved Methods for Digital Measurement of Torsional Vibration", SAE paper no. 962204, 1996

Measurement and Analysis of Rotational Vibration and other Test Data from Rotating Machinery.
Seán Adamson, Rotec GmbH, Munich.
From SAE World Congress, Detroit 2000.
SAE Paper No. 2000-01-1333.

The Effects of Belt Error on Sound and Vibration

Paul A. Piorkowski, Michael Pierz, GM Powertrain, Ypsilanti, USA
Karl–Rainer Feuring, Rotec GmbH, Munich

Abstract

Belt error is the rotational speed relationship across a sheave set. We measure the change in the rotational speed between the primary and secondary sheave. The error is put in an order relationship to the input and output sheave. Simultaneously a measurement is made of belt pass speed, sound pressure and vibration. This testing is conducted with a push type segmented belt in a semi-anechoic test cell with dynamometers driving and loading the sheave set. Testing will be conducted varying clamping force with selected ratios and loads. A comparison is made between the indicated channels and conditions. Analysis is performed using order, Hz and waterfall plots. In closing we outline the relationship between belt error and sound and vibration.

Keywords

Belt Error (Slip)
Order Tracking
Order Cut
Waterfall
Resonance

1. Introduction

The purpose of this paper is to outline the techniques needed for the measurement of Belt Error and then to understand it's Impact on sound and vibration. First we must define Belt Error, this phenomena is the difference in speed between the sheaves taking in to account the selected ratio. This change in speed (the secondary sheave slowing down and speeding up as referenced to the primary sheave) is Belt Error. Belt Error is important to define as it can have a negative impact on the sound and vibration characteristics of transmissions

2. Order Tracking

Typically when performing analysis on microphone and vibration data, Order Tracking is the preferred method for extracting the data that relates to a signal component. This method is also known as an Order Cut which utilizes only the sound data that relates to a chosen order and is tracked off the input or output speed (see illustration 1). Unfortunately this method can not be applied to the tracking of a CVT belt or chain since the belt ratio changes and does not have a constant order relationship to either input or output speed. A different method must be found to provide component specific data for the CVT belt, so the transmission error method was used.

3. Test Setup & Instrumentation

This CVT transmission testing was conducted with a push type segmented belt in a semi-anechoic test cell with dynamometers driving and loading the sheave set.

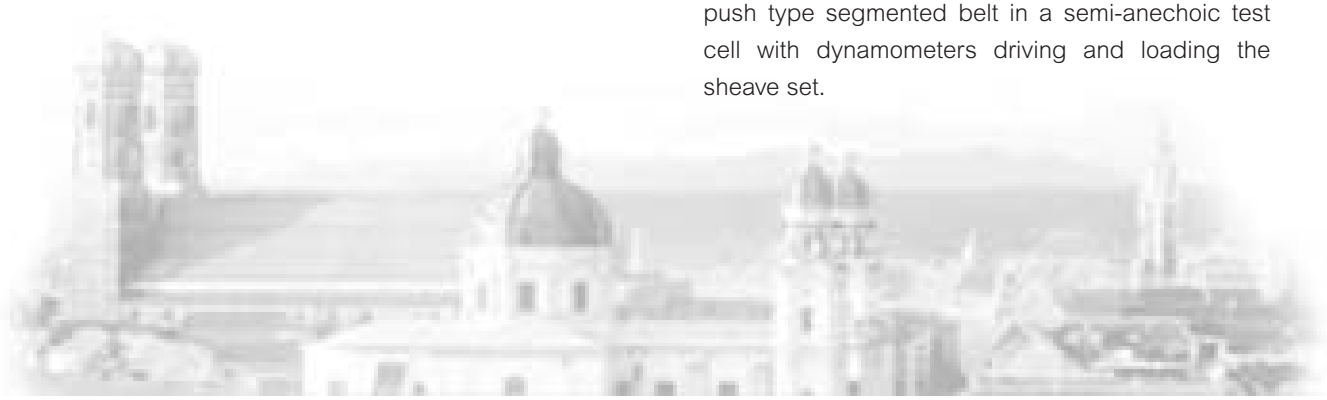

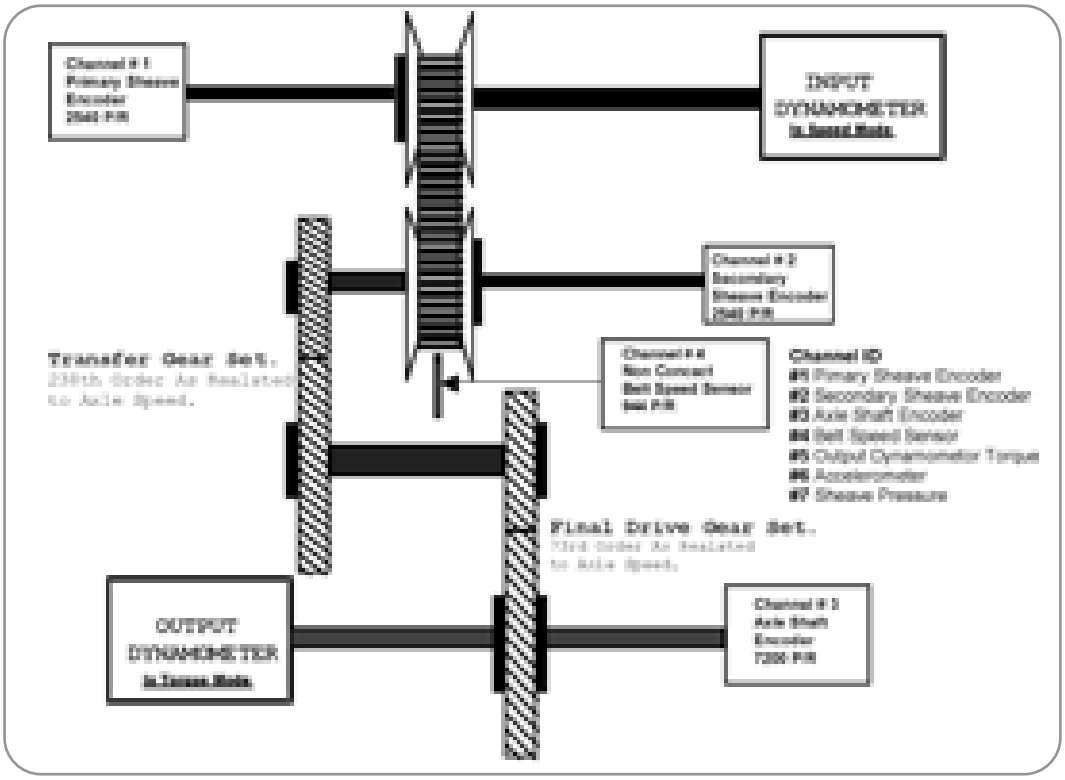

Figure 1 *Belt Error Test Schematic*

Microphones were placed 1 meter from transmission and accelerometers were mounted on the case. Encoders were mounted on the primary sheave, secondary sheave, and the transmission output. Sheave pressure and output dynamometer torque were also measured as data channels. A non-contact pickup was used to track belt speed. The input dynamometer was controlled in speed mode and the output dynamometers were controlled in torque mode.

The belt pass signal was acquired by using a multi-coil active sensor. These sensors are available as two, four, or eight coil pick-ups. A specially modified belt was used to accommodate the requirements of the sensor. Since belt segment thickness closely matched the coil spacing of a four-coil sensor, it was selected. To provide a clear signal, every second segment of the belt was removed and replaced with a modified segment with approximately 0.75-mm of the segment ground off. The resulting combination of multiple sensor coils and belt segments provided 976 pulses per belt pass. An additional modified belt was produced which did not mechanically modify the belt. Again every other segment was modified, but this time a chemical conversion coating was applied to the top surface of the segments. This coating on the assembled belt provided an alternating contrast pattern for use with a laser pulse tachometer.

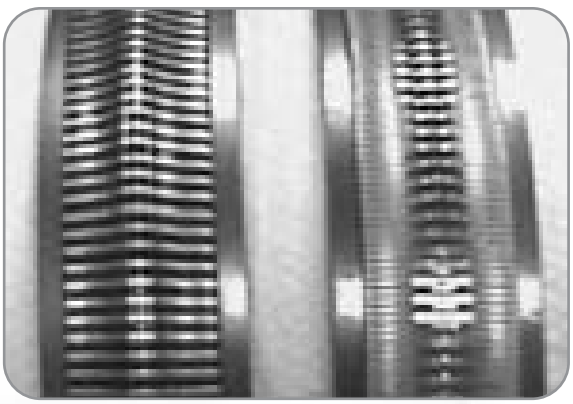

Figure 2 *Belts (Optical L, Four Coil R)*

While the belt produced for use with the laser tachometer could produce a reliable speed signal for the belt, the resolution was half of the total number of belt segments. Because of this limited resolution, the laser method could only be used for orders of less than 1/4 of the belt pass order. Sheave related phenomenon occurring relative to the belt could be sensed with the laser tachometer, but in order to sense effects related to segments, only the four-coil sensor could be used.

3.1 Data Acquisition

All data was recorded using a Rotec USA system with six speed, and sixteen analog input channels. All channels were recorded at 100MHz using a synchronized clock, eliminating phase errors. All non-speed channels, (analog) were down sampled at 8192 kHz.

The digital measurement technique for high resolution measurement of rotational speeds requires attachment of rotary encoders to the shafts. The instantaneous frequency of the pulse train is proportional to the instantaneous angular velocity of the shaft. The elapsed time from the start of the measurement for each encoder increment passing is measured using a 32-bit long, 10 ns clock frequency counter / timer. The average shaft speed during the passage of each tooth is calculated by dividing the angular separation for each tooth pass by the elapsed time. The measuring step is the angular value corresponding to the distance between two consecutive edges of the square wave TTL signal from the speed measurement. The instantaneous rotational speed is then calculated by multiplying the time intervals with the line count of the rotary encoder.

A pair of sheaves should transmit rotary motion uniformly from the drive shaft to the driven shaft. Transmission error testing investigates the rotational movement of the axes of a pair of shafts and numerically describes the irregularities in transmission (Transmission Error). The transmission error curve results from the deviation in rotating angle between the two en-

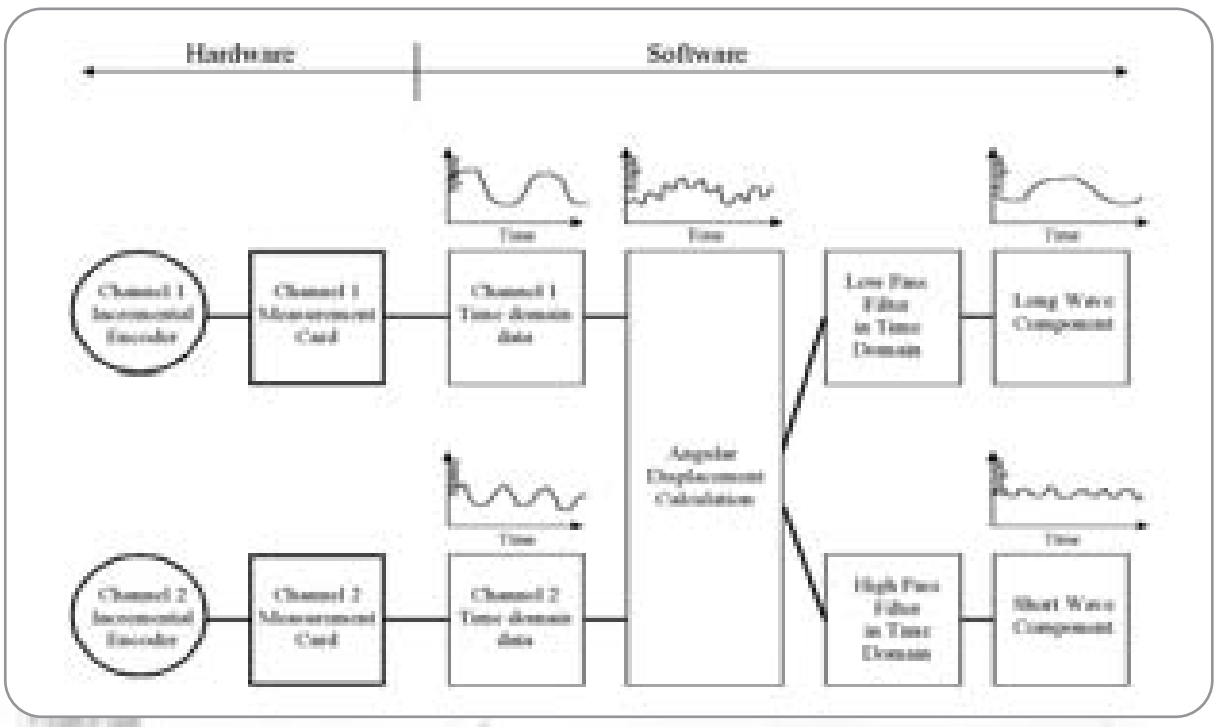

Figure 3 *Hardware and Software Schematic*

coders. The patterns in the transmission error curve originate from eccentricity in rotation of the drive and the driven shafts and from the slippage or deformation of belt segments. This is observed in the form of a fairly regular once-per-tooth pattern superimposed on large waves, which are related to once-per-revolution type errors.

The once-per-segment (or faster) short wave components of the curve, result from slip or deformation caused by surface structure effects and segment geometry. The long wave portion is due to run-out errors. Additionally, components due e.g. to support structure bolts may be present which bear no relationship to the sheave interface geometry.

In order to get a complete picture of the systems running behavior, it is recommended that data be recorded for one complete over-rolling of the two wheels. The total transmission error signal may be divided into long wave and short wave components. The long wave portion of the total error curve is obtained by using a low pass digital filter. The short wave portion is obtained by high pass filtering of the total error curve. The cut-off order in both cases is set at 1/3 tooth mesh.

4. Test Results

Data was acquired from a transmission with the four-coil sensor and reduced to determine belt error. The error, in terms of angular displacement showed the expected characteristics of short and long wave components. Further analyses of the data were performed to determine order content of the signal produced by the belt.

In order to determine the order content of the signal a FFT of the total signal is performed. A plot of the output after the FFT has been performed shows the order content of the signal. The example plots shown

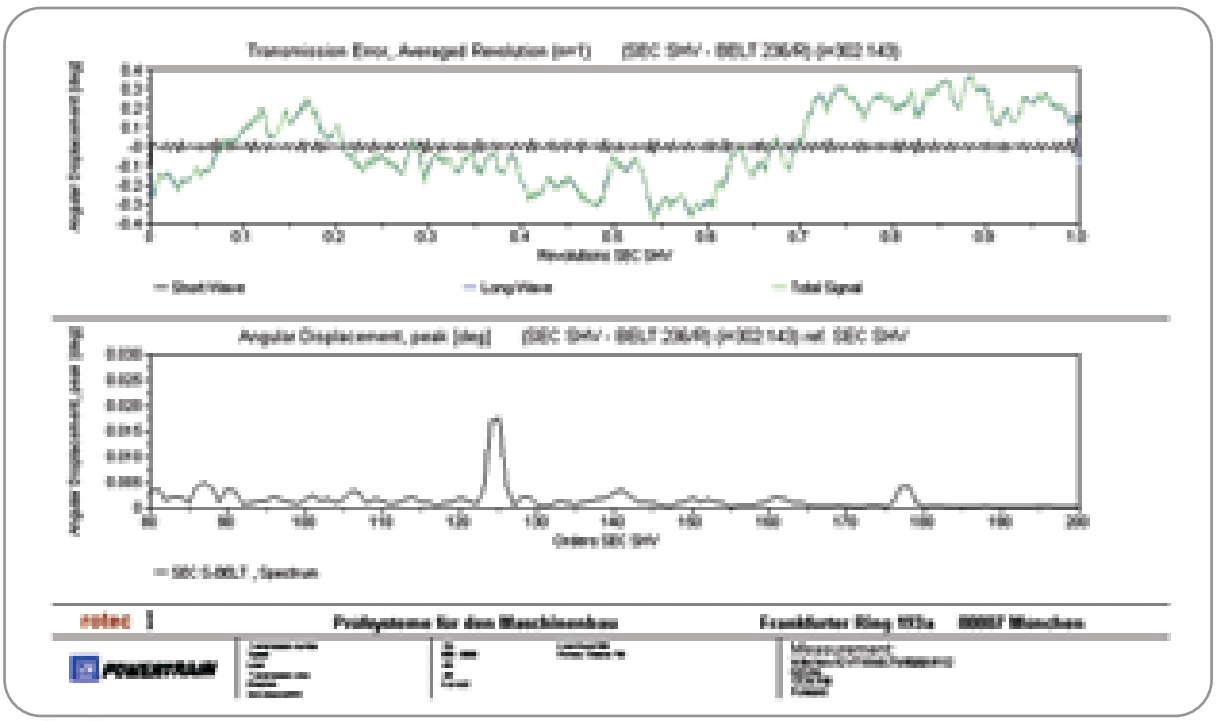

Figure 4 *Typical combined Error and order Plot*

in Figure 4 show a typical output from the analysis. The upper plot shows the long and short wave components of the signal separated for a driven sheave and belt. The lower plot is the FFT output showing a portion of the order content of the total signal.

While tests were run with the laser tachometer, it was not possible to determined disturbances in the range of segment pass because of a lack of resolution. Similarly, with the four-coil sensor, the signal is attenuated significantly as the order of interest approaches half the number pulses of either the belt or sheave in question. This effect can be clearly seen in Figure 5. While disturbances should be present at orders above 180 of the secondary sheave, there is only a negligible signal present. With an eight-coil sensor the useful order range would be doubled.
Within the range of useful signal possible with this test setup, significant conclusions can be drawn. In Figure 5, the load was swept and speed held constant during the acquisition of data. The peak shown at order 124 is the result of segment pass on the sheave and the minor peak at 178 is a result of torsion resonance in the system. Similarly in Figure 6 orders are shown for the same components but under constant torque loading. Under constant torque the significant disturbance at the segment pass order is not present.

Using this technique with the other data channels that were simultaneously recorded, causal relationships can be determined with the observed sound and vibration signals. Figure 7 illustrates the relationship of Sound Pressure to the previously identified belt order. The order plot shows the 125 order and it's harmonic in the microphone data. The sound pressure data shows the same order relationship as the belt error plots, but with

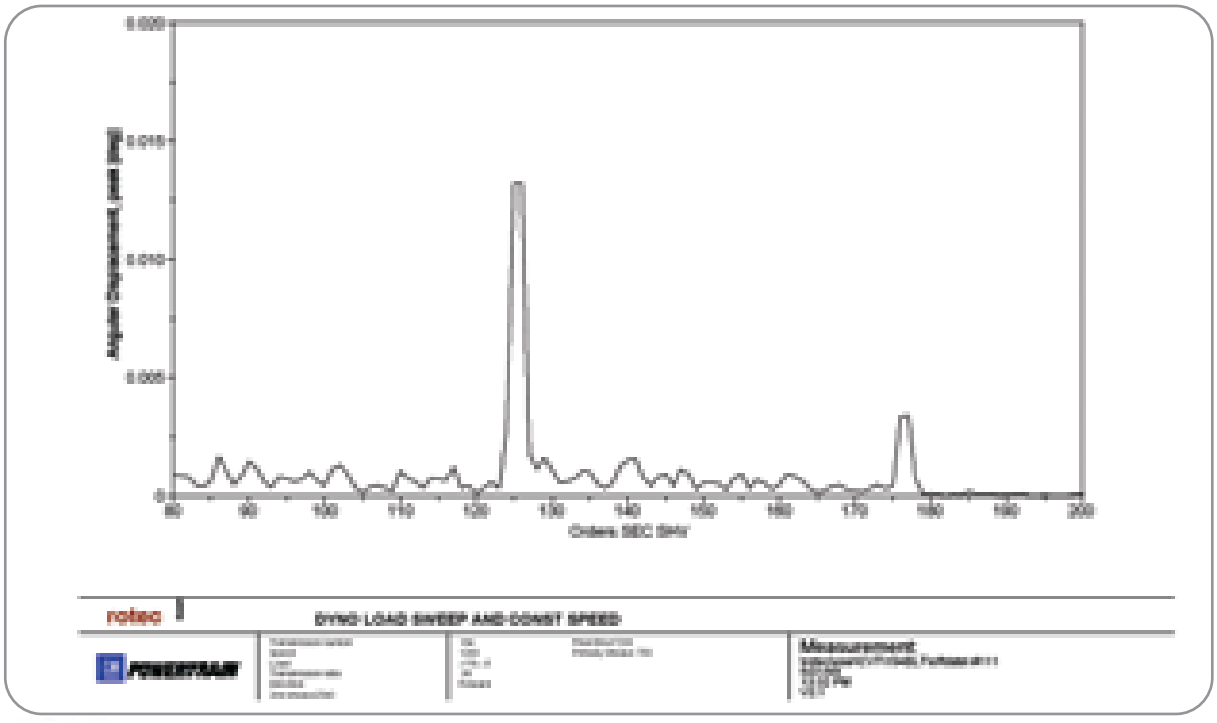

Figure 5 *Order Plot for Modified Belt with Four-Coil Sensor Load Sweep*

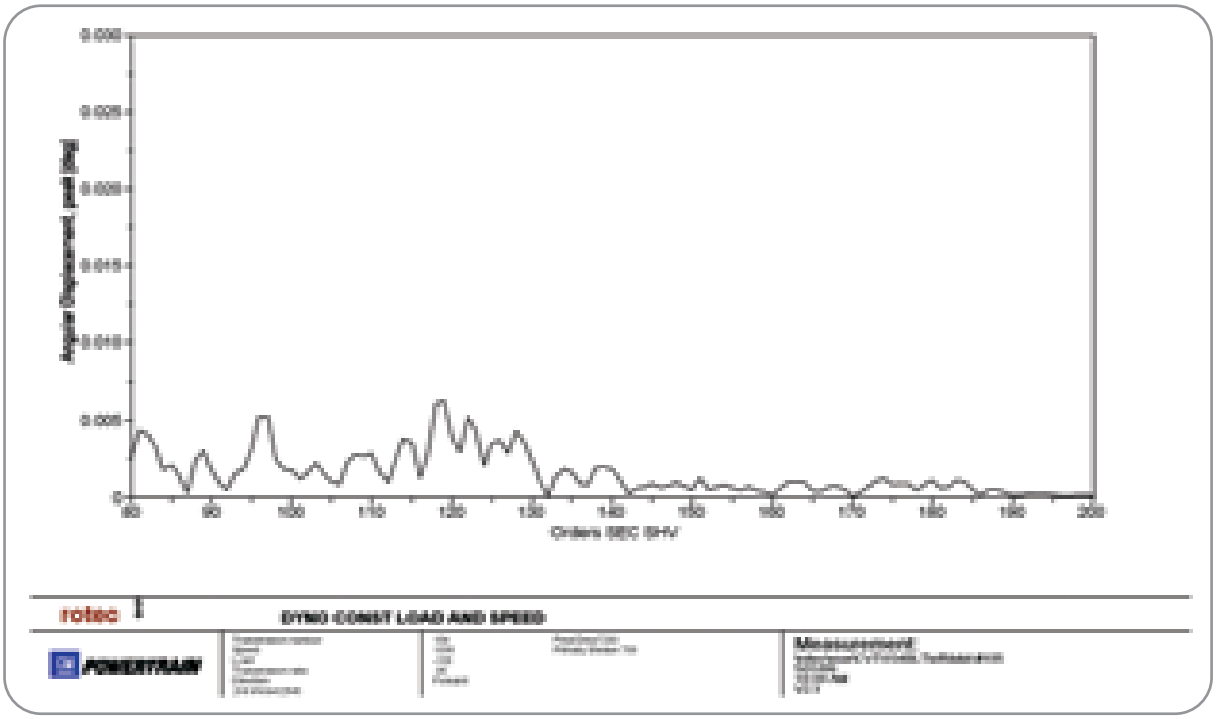

Figure 6 *Order Plot with Constant Load and Speed*

higher orders present. The higher harmonic shown in the sound data is probably present in the belt error, but because of the limited resolution possible with the sensor used for belt speed, not detectable in the error plot. Pressure signals relating to sheave clamping force can be analyzed in the same way to determine if the disturbance occurring under changing load is propagated through the hydraulic circuit.

5. Conclusion

Transmission error is a powerful tool for the analysis of CVT belt and sheave systems. Use of TE data to identify and quantify Orders under varying operating conditions simplifies the identification of causal relationships for various noise and vibration sources.

The relationship of belt to sheave relative displacement shown by transmission error analysis is affected by the rate of torque change; speed change and clamping pressure. The development of more accurate sensing methods will allow the more complete investigation of these relationships. The sound pressure data indicates a significant harmonic of the segment pass order is present. Amplitude damping of the error signal because of the low ratio of pulses to segments prevents the higher harmonic signal from being detected in the current test setup.

Future work with belt error should encompass testing with higher resolution belt and sheave encoders to allow higher harmonics of the error signal to be detected. The insights into the physical system responsible for producing noise and vibration will allow improvements to be made which will ultimately lead to greater customer satisfaction.

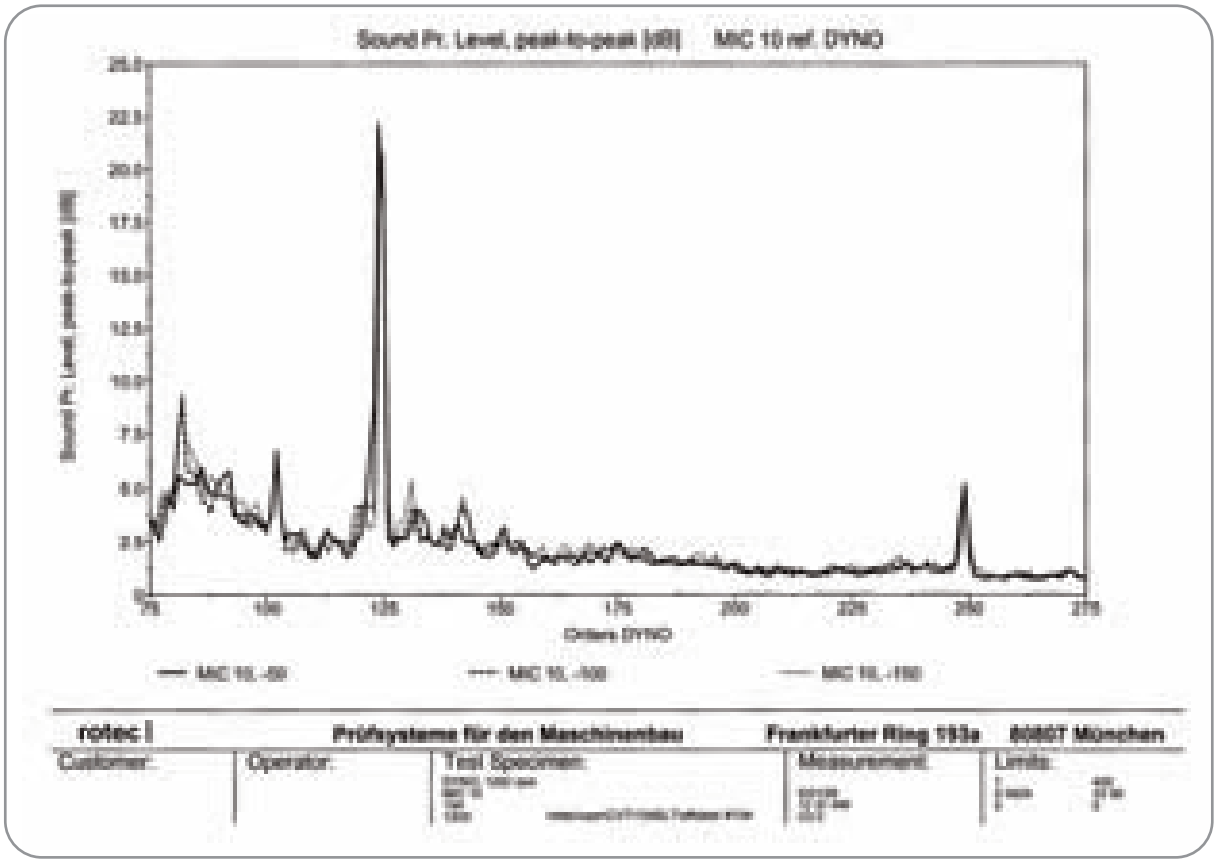

Figure 7 *Sound Pressure Order Plot*

7. Acknowledgments

We Gratefully wish to acknowledge Karl Janovits and the Transmission Engineering Staff at GM Powertrain, Tom Mitchell and the GM Powertrain Integration Engineering Center, The technicians at the Romulus Engineering Center and the Staff at Rotec Gmbh. Without their help this work would not have been possible.

In the interest of product security data presented in this report has been scaled and does not reflect the actual observed values.

The Effects of Belt Error on Sound and Vibration. Paul A. Piorkowski and Michael Pierz, General Motors Powertrain, Ypsilanti, USA. Karl-Rainer Feuring, Rotec GmbH, Munich.

Presented at the International Congress on Continuously Variable Power Transmission CVT'99. Eindhoven, The Netherlands, Sept. 16–17, 1999.

rotec GmbH
Prüfsysteme für den Maschinenbau
Joseph-Dollinger-Bogen 18
D-80807 Munich, Germany
Tel: +49 (0) 89 323 651 - 0
Fax: +49 (0) 89 323 651 - 56
www.rotecmunich.de
info@rotecmunich.de